Development Advance Online Articles. First posted online on 11 October 2016 as 10.1242/dev.122721
Access the most recent version at http://dev.biologists.org/lookup/doi/10.1242/dev.122721

RESEARCH ARTICLE TECHNIQUES AND RESOURCES

Caspase-mediated apoptosis induction in zebrafish cerebellar Purkinje neurons

Weber,T[1,2,6,#]; Namikawa, K[1,#]; Winter B[1], Müller-Brown K[1], Kühn, R[2,7]; Wurst, W[2,3,4,5]; Köster,R. W.[1,*]

[1]TU Braunschweig, Zoological Institute, Cellular and Molecular Neurobiology, Spielmannstr. 7, 38106 Braunschweig, Germany.

[2]Helmholtz Zentrum München, German Research Center for Environmental Health, Institute of Developmental Genetics, Ingolstädter Landstr. 1, 85764 Neuherberg, Germany.

[3]Deutsches Zentrum für Neurodegenerative Erkrankungen e. V. (DZNE), Standort München, Feodor-Lynen-Str. 17, 81377 München, Germany.

[4]Munich Cluster for Systems Neurology (SyNergy), Feodor-Lynen-Str. 17, 81377 München, Germany,

[5]Technische Universität München-Weihenstephan, Lehrstuhl für Entwicklungsgenetik, c/o Helmholtz Zentrum München, Ingolstädter Landstr. 1, 85764 Neuherberg, Germany.

[6]Current address: University Medical Center Göttingen, Department of Child and Adolescent Health – Division of Neuropediatrics, Robert-Koch-Str. 40, 37075 Göttingen, Germany.

[7]Current address: Max-Delbrück-Centrum für Molekulare Medizin, Robert-Rössle-Str. 10, 13125 Berlin, Germany.

[#] these authors contributed equally

*Corresponding author: r.koester@tu-bs.de

Key words: zebrafish, cerebellum, Purkinje cells, cell ablation, apoptosis, inducible Caspase,

SUMMARY STATEMENT

Tamoxifen-induced Caspase activation is established in zebrafish to trigger fast and efficient Purkinje cell ablation via apoptosis.

ABSTRACT

The zebrafish is a well-established model organism to study *in vivo* mechanisms of cell communication, differentiation and function. Existing cell ablation methods are either invasive thereby creating additional tissue damage and potential infection sites, or they rely on the cellular expression of prokaryotic enzymes and the use of antibiotic drugs as cell-death-inducing compounds. We have recently established a novel inducible genetic cell ablation system that is based on Tamoxifen-inducible Caspase8-activity, thereby exploiting mechanisms of cell death intrinsic to most cell types. Here we prove its suitability *in vivo* by the ablation of cerebellar Purkinje cells (PCs) in transgenic zebrafish, which coexpress the inducible Caspase and a fluorescent reporter to monitor ablation processes. Incubation of larvae in Tamoxifen for 8 hrs activated endogenous Caspase3 and cell death, while incubation for 16 hrs led to the nearly complete loss of PCs by apoptosis. Using live confocal imaging, we observed synchronous cell death autonomous to the PC population and phagocytosing microglia in the cerebellum, reminiscent of developmental apoptosis in the forebrain. Thus, induction of Apoptosis Through Targeted Activation of Caspase by Tamoxifen (ATTAC™) further expands the repertoire of genetic tools in zebrafish for conditional interrogation of cellular functions.

INTRODUCTION

In vivo cell ablation is a useful research method to study the development, function, interaction and regeneration of cells or tissues in a multicellular context. Working with zebrafish embryos, one can combine *in vivo* cell ablation with multicolor live imaging techniques and numerous forms of genetic or pharmaceutical manipulations due to the aquatic life style, small size, external development and transparency of these embryos (Lieschke and Currie, 2007; Weber and Köster, 2013). To obtain spatial and temporal control over the cell type to be ablated, and to avoid collateral tissue damage associated with invasive ablation techniques, inducible genetic cell ablation methods were developed. Cell type specific or subcellular-specific expression of the phototoxic fluorescent protein KillerRed (KR) (Bulina et al., 2006) or SuperNova (Takemoto et al., 2013) can be used to generate radicals upon excitation either resulting in cell death or destruction of the targeted organelle (Teh et al., 2010; de Anda et al., 2010; Korzh et al., 2011). Its use though

is restricted to tissues accessible by the often shallow light penetration. Expression of the bacterial enzyme nitroreductase (NTR) does not require light but prodrug uptake of the expressing tissue to elicit induction of cell death through enzyme mediated prodrug conversion into a p53-independent DNA damaging compound. (Cui et al., 1999; Djeha et al., 2005). Depending on the prodrug used, cell death will be restricted to the NTR-expressing cell population as is the case for the antibiotic metronidazole (MTZ). Alternatively with the prodrug CB1954, NTR non-expressing neighbouring cells are killed by a spread of the toxic compound, a process called bystander effect which is desirable in cancer therapy applications (Bridgewater et al., 1997; Djeha et al., 2005; Lipinski et al., 2006). NTR-mediated metronidazole-induced cell ablation has been widely used in zebrafish in several tissues including rod photoreceptors, pancreatic **β**-cells and hepatocytes (Curado et al., 2007; Davison et al., 2007; Pisharath, 2007; Chen et al., 2011; White and Mumm, 2013). An even improved NTR-variant with faster kinetics was recently reported in zebrafish increasing the effectiveness and versatility of this ablation system (Mathias et al., 2014).
If two cell types are to be ablated independently though, a second, NTR-independent ablation system is necessary. It is desireable to complement existing methods by a cell ablation system available in zebrafish that directly activates apoptosis as a non-lytic endogenous cellular mechanism of cell death and that uses well-established drugs with high activity in almost all tissues.
The small synthetic compound FK1012 can trigger the homotypic dimerization of a fusion protein of the FKBP dimerization domain and the initiator caspase Caspase8. Thereby apoptotic cell death is activated, a method termed **A**poptosis **T**hrough **T**argeted **A**ctivation of **C**aspase8 (ATTAC) (Pajvani al., 2005). The pharmacology of the ligand though is unknown and harbors an immunosuppressive activity. In analogy to this method, we have recently shown that Caspase8 fused to the mutated Tamoxifen-interacting estrogen receptor ligand binding domain (ER^{T2}) can be activated by Tamoxifen to induce apoptosis in a wide range of different cultured cell types that express this „inducible caspase“ (Chu et al., 2008). In the past, Tamoxifen has been proven to activate protein function in tissues of all germ layers in aquatic vertebrates and mammalian model organisms. It works in embryos and adults and passes the blood brain barrier. Tamoxifen is an estrogen analogue, but the

three known estrogen-receptors found in zebrafish do not respond to Tamoxifen (Bardet et al., 2002).

We have now transferred this ablation system to living zebrafish pairing it with the coexpression of a fluorescent protein to monitor the time course and extent of ablation. We targeted differentiating cerebellar Purkinje cells (PCs) as they display a highly polarized morphology and form a single cell layer allowing for a good score of their survival and healthiness and easy bioimaging (Hibi and Shimizu, 2012). Moreover, PCs are the sole output neurons of the cerebellum, which are affected by several degenerative diseases (Fernandez-Gonzalez et al., 2002). This transgenic PC- ATTAC™ (ATTAC induced by Tamoxifen) zebrafish strain will thus be a powerful tool to study the consequences of PC ablation with respect to cerebellar neuronal survival, regeneration and function in the near future.

RESULTS

Inducible Caspase under transient transgenic conditions

Tamoxifen is usually dissolved in ethanol (EtOH) and used in zebrafish at concentrations of 5 μM (Mosimann et al., 2011). In order to address whether EtOH or Tamoxifen-treatment alone induces cell death, zebrafish embryos were incubated in these solutions for ten hours starting at 24 hpf using staurosporine as positive control (Fig. S1A). Acridine Orange (AO) staining detected a seven-fold increase in the number of dead cells upon staurosporine treatment while neither EtOH nor Tamoxifen incubation resulted in elevated cell death compared to non-treated wild type embryos (Fig. S1B). Next, heterozygous Tg(*her3*:*KalTA4*) transgenic embryos with KalTA4 (a zebrafish optimized Gal4-variant) expression in cells of the ventral spinal cord were injected at the one-cell stage (Babaryka et al., 2009) with a 5xUAS:FyntagRFP-T-T2A-Caspase8ER^{T2}-expression vector coexpressing the membrane bound fluorescent protein FyntagRFP-T together with Caspase8ER^{T2} linked by a self-cleaving T2A-peptide (Kim et al., 2011). At 24 hpf these embryos showed transgene expression throughout the ventral spinal cord allowing for Acridine Orange (AO) staining for cell death analysis (Fig. S2A).

Elevated levels of cell death in cells along the ventral spinal cord could be observed in EtOH-treated control specimens as indicated by AO staining (Fig. S2B 5th row), such elevation in cell death could not be found with FyntagRFP-T expression alone (Fig. S2B bottom row). Tamoxifen-incubation of inducible caspase expressing embryos starting at 24 hpf strongly increased cell death already after 4 hours (Fig. S2B 1st, 2nd row) reaching highest level at about 8 hours of incubation in Tamoxifen (Fig. S2B 4th row). Image recording of these cells using a confocal laser scanning microscope (CLSM) revealed that cell death strictly localized to FyntagRFP-T/Caspase8ER^{T2}-coexpressing cells (Fig. S3A) with 25.3% (±3.5% SD) of transgene expressing cells entering cell death already without Tamoxifen-treatment and clearly above background compared to 5xUAS:FyntagRFP-T expressing control cells. Importantly, cell death was significantly increased up to 89.1% (±11.5% SD) of all transgene expressing cells upon 8 hours of Tamoxifen-treatment (Fig. S3B). This shows that the activity of the Caspase8ER^{T2}-fusion protein is leaky under transient transgenic conditions, but that its acitivity can be strongly induced by Tamoxifen-treatment resulting in cell death of the vast majority of all transgene-expressing cells within a time-window of 8 hours.

To show that other than ventral spinal cord cells can be driven into apoptotic cell death (Fig. S4A) immunostainings against activated Caspase3 were performed in 5xUAS:FynVenus-T2A-Caspase8ER^{T2}-injected embryos expressing KalTA4 either in rhombomere 3 and 5 (Et(*shhb:KAlTA4,UAS-E1b:mCherry*)hzm6Et) (Fig. S4B) or in skeletal muscle (Et(*shhb:KAlTA4,UAS-E1b:mCherry*)hzm8Et) (Fig. S4C). Again while in EtOH-treated control fish elevated levels of apoptosis were detected (Fig. S4 upper rows) likely due to leakiness of Caspase8ER^{T2}-activity, apoptotic cell death was significantly induced upon 6 hours of Tamoxifen-treamtent (Fig. S4 lower rows).

Establishment of stable transgenic PC- ATTAC™ fish

To address whether the leakiness of Tamoxifen-inducible Caspase8-ER^{T2} activity in the absence of Tamoxifen (Fig. 1A) exists under stable transgenic conditions we established a zebrafish strain coexpressing the membrane bound fluorescent protein FyntagRFP together with Caspase8ER^{T2} linked by a self-cleaving T2A-peptide (Fig. 1B) (Kim et al., 2011). To achieve specific expression in differentiating cerebellar Purkinje cells (PCs) a regulatory

element isolated from the upstream region of the zebrafish *carbonic anhydrase 8* homolog was used (Matsui et al., 2014) resulting in the stable transgenic zebrafish strain Tg(*ca8:FMA-TagRFP-2A-casp8ERT2*)^{bz11Tg} (Fig. 1C) which we named PC- ATTAC™ according to the previously used nomenclature (Pajvani et al., 2005) but pointing out its Tamoxifen-dependence.

Whole mount mRNA *in situ* hybridization against *tagRFP* at 4dpf confirmed transgene expression only in the differentiating cerebellum (Fig. S5). Next, PC- ATTAC™ larvae of the F2 and F3 generations were analyzed *in vivo* by CLSM. First red fluorescent cerebellar cells could be observed around 3 days postfertilization (Fig. S6A, B), which formed the wing-like structures characteristic for the two cerebellar hemispheres (Fig. S6B). PCs are GABAergic and the gene encoding the *pancreas transcription factor 1a* (*ptf1a*) is transiently expressed in precursors of GABAergic neurons of the cerebellum. Therefore its enhancer drives the expression of GFP in Purkinje cell progenitors and other cerebellar interneurons (Fig. S6 A, B) (Lin et al., 2004; Hibi and Shimizu, 2012). When we crossed PC- ATTAC™ carriers with the transgenic reporter line Tg(*ptf1a:egfp*), all red fluorescent cells analysed were marked by cytoplasmic co-expression of green fluorescence (Fig. S6B white arrows), supporting their normal development from *ptf1a*-expressing embryonic progenitor cells. To confirm the specific expression of inducible Caspase8 in PCs, we performed double-immunohistochemistry stainings using whole mounts of 5 dpf old transgenic larvae and antibodies against tagRFP and the PC-specific ZebrinII antigen respectively (Lannoo et al., 1991). Indeed, we found that all red fluorescent cells coexpressed ZebrinII, proving their identity as PCs (Fig. 1D). Concomitant Caspase8ER^{T2}-expression was confirmed by Western blot analysis (Fig. 1G) and immunohistochemistry using an anti-Caspase8 antibody demonstrating that Caspase8 expression is confined to FyntagRFP expressing cells (Fig. 1E). Because tagRFP is fused at its N-terminus with the myristinylation site of the Fyn-kinase, axons, somata and the prominent dendrites of PCs could be observed in detail (Kameda et al., 2008) including the long axonal projections of PCs forming the cerebello-octavolateralis tract to vestibular nuclei (Bae et al., 2009; Matsui et al., 2014; Biechl, et al., 2016) (Fig. 1F, white arrowheads). These axonal projections did not show any signs of degeneration, fragmentation, abnormal projection or sprouting. Neither did homozygous F3-larvae, which are easily detectable by their brighter fluorescence, show any signs of altered PC-

morphology (not shown) suggesting that the inducible Caspase8 was inactive in larvae of the PC- ATTAC™ strain in the absence of Tamoxifen.

Tamoxifen-induced PC-death in PC- ATTAC™ fish

In order to test the PC-death inducing properties of the Caspase8, heterozygous PC-ATTAC™ larvae with a red fluorescent PC layer were treated with the active form of Tamoxifen, 4-hydroxy-Tamoxifen (4OHT), diluted in 0.5% EtOH starting at 4 dpf (Goetz et al., 2008). $5x10^{-6}$M 4OHT – a concentration that lies in the range of other 4OHT-mediated application protocols in zebrafish (Hans et al., 2009; Kroehne et al., 2011; Mosimann et al., 2011) - induced widespread ablation of PCs. Cell ablation was evident by the formation of massive PC debris visible after 16hrs (Fig. 2A). Strikingly, the extensive dendritic layer of PCs was completely disrupted (Fig. 2B, white arrowheads), somata were replaced by round cell debris (Fig. 2B insets) and the projections forming the cerebello-octavolateralis tract were fragmented (Fig. 2A yellow square). These findings show that the Caspase-mediated PC ablation achied by 4OHT incubation for 16 hrs at the concentration of 5µM is both effective and highly efficient *in vivo*.

PC-ablated specimens returned to 4OHT-free rearing medium at this time point were reanalyzed 24, 48 and 72 hours after 4OHT-treatment (8, 32, and 56 hours after removal of 4OHT, respectively). Still red fluorescent PC debris could be detected although to a lesser extent but being widely distributed throughout the larval cerebellum (Fig. 2C). This shows that PCs were not able to quickly recover but had been irreversibly removed and were unable to escape cell death. This indicates that 4OHT-treatment resulted in the fast induction of PC-death through the activation of Caspase8, and was therefore likely mediated by apoptosis.

Lower concentrations of 4OHT (10^{-6}M) induced only mosaic cell death or „dendritic damage“, which was associated with locally confined dot-like disruptions of the otherwise smooth texture within dendritic compartments of PCs as well as debris nearby somatic membranes (not shown). Treatments with such a lower concentration of 4OHT might be of interest if neuronal cell damage rather than the consequences of cell death are in the focus of interest e.g. when studying the plasticity or the regrowth and remodelling of PC dendrites. Larvae treated in Tamoxifen-free medium that contained only the diluent EtOH

showed no signs of damage in the PC layer (Fig. 2A, B) further confirming that Caspase-activity in PC- ATTAC™ larvae is not leaky but can be well controlled.
Potentially, Caspase8 could be active at low levels in the absence of Tamoxifen or Caspase8-activity could be induced by endogenous estrogen signaling. This would result in slow but continuous PC death accumulating over time. As there is currently no evidence for Purkinje cell progenitor proliferation in adult zebrafish (Kaslin et al., 2013), such leaky Caspase8-activity would result in progressive gaps in the PC layer of the adult zebrafish cerebellum. Sagital sections of the cerebellum from adult PC- ATTAC™ zebrafish revealed no such gaps but a continuous PC layer without signs of progressive PC degeneration further excluding a leaky Caspase8-activity (Fig. S7). These findings show that in the established PC- ATTAC™ strain Caspase8ER^{T2} is inactive but can be triggered reliably by Tamoxifen to induce cell death specifically in cerebellar PCs.

Dynamics of PC ablation in PC- ATTAC™ larvae

To be able to score the success of our ablation system numerically, we counted the PCs that expressed tagRFP in PC- ATTAC™ larvae from confocal z-stacks of the right cerebellar hemisphere at 4 dpf, when ablation was usually induced in this study. We counted an average of 131.3 cells (STD 22.4; n=11) per hemisphere, indicating that the Purkinje cell population encompasses roughly 260 cells at this developmental stage, which is not increasing dramatically in number over the subsequent days (Fig. S8) (Hamling et al., 2015).
Caspase3 acts as an executing caspase downstream of Caspase8. To clarify that PC death indeed occurs by apoptosis and to determine the time-course of cell death heterozygous PC-ATTAC™ larvae were treated at 4 dpf with 4OHT and processed in 2 hour-intervals for activated (cleaved) Caspase3 immunohistochemistry. EtOH-controls at 0 and 8 hours of 4OHT treatment (Fig. 3F, G) showed background levels of cells with activated Caspase3 similar to PC-ATTAC™ larvae at the onset of 4OHT-treatment (0.6 cells on average at 0hrs) (Fig. 3A)
A first significant elevation of apoptosis in PC- ATTAC™ larvae could be observed after 6 hours of 4OHT-treatment in about 6.6% of all FyntagRPF-expressing PCs (17.1/260, n=7 larvae; Fig. 3C, H) based on previously determined cell numbers of 260 PCs at 4 dpf. After 8 hours of 4OHT-treatment these levels increased to 22% (58.6/260, n=8 larvae) and

subsequently declined to 6.6% (17.2/260, n=6 larvae) and 2.8% (7.4/260, n=5 larvae) after 10 and 16 hours of 4OHT-incubation respectively (Fig. 3D, E, H). This shows that the induction of apoptosis is fast occurring synchronously within a few hours. The low percentage of PCs containing activated Caspase3 compared to widespread fragmentation of the PC layer after 16 hours of 4OHT-treatment suggests that activated Caspase3 staining is only transient in dying PCs. Activated Caspase3 staining always colocalized with FyntagRFP expression confirming that only PCs were driven into apoptosis.

To better score the extent of PC ablation we performed 4OHT-treatments for 16 hours with heterozygous 4 dpf PC- ATTAC™ larvae and waited after 4OHT-washout for another 24 hours to allow for completion of cell death. Subsequently these embryos were subjected to both RT-PCR analysis to detect remaining *fyntagRFP* expression and mRNA *in situ* hybridization against *carbonic anhydrase 8* (*car8*) as Purkinje cell specific marker not only in adult but also in larval zebrafish (Namikawa et al., in preparation). RT-PCR from isolated heads showed strongly reduced amounts of remaining *fyntagRFP* mRNA compared to EtOH controls (Fig. 3I). In addition, while *car8*-expression was prominent across the cerebellum in EtOH controls, virtually no *car8*-expression was visible in PC-ablated specimens (Fig. 3J). Finally, counts of PCs 2 and 5 days post-treatment (dpt) revealed a reduction of PCs to about 10% compared to PCs quantified in EtOH-controls (Fig. 3K, n=5 larvae counted per time point). This value may even underestimate the efficiency of ablation, as PC progenitors that did not express Caspase8 yet during 4OHT-treatment and that differentiated into fluorescent PCs after 4OHT-removal could counteract diminishing PC numbers. These findings demonstrate that 16 hours of 4OHT-treatment of heterozygous PC- ATTAC™ larvae resulted in nearly complete elimination of the entire cerebellar PC population. Thus cell ablation in PC- ATTAC™ larvae is not only fast but also efficient.

Acute Caspase8-mediated apoptosis does not spread to PC connecting neurons

An interesting question is whether PC apoptosis will affect the immediate health and survival of afferents or efferents for example due to the loss in physiological connectivity with PCs. The most prominent and numerous direct afferents of PCs are cerebellar granule cells (GCs), while eurydendroid cells (ECs) are the only efferents of PCs (besides the cerebello-octavolateralis tract projecting to vestibular nuclei) (Fig. 4A). GCs are marked by

EGFP fluorescence in the line Tg(*gata1:egfp*) (strain 781), (Long et al., 1997; Volkmann et al., 2008), while ECs express EGFP in the Tg(*olig2:egfp*) strain (Park et al., 2002). Thus PC-ATTAC™ carriers were crossed with carriers of these different transgenic backgrounds and double transgenic larvae were subjected to 16 hours of 4OHT-treatment at 4 dpf to induce PC ablation.

gata1:EGFP-expressing GCs as well as their axonal projections - the parallel fibers - did not show any signs of fragmentation or cell death neither in both EtOH controls (Fig. 4B) nor in 4OHT-treated specimens (Fig. 4C). Similarly, the somata of *olig2*:EGFP-expressing eurydendroid cells were arranged in their expected pattern without signs of cell death (Fig. 4D) that could neither be observed in the following days during removal of PC debris (Fig. S9).

Taken together, these data show that direct PC afferents or efferents are not obviously affected in their morphology, health or survival shortly after 4OHT-induced PC ablation. However, as these cerebellar neurons are integrated into circuits containing PCs, the electrophysiological input or output of these PC afferents and efferents is lost upon PC apoptosis. Whether such interruption of cerebellar connectivities – where PCs take a central role – and the loss of electrophysiological coupling will result in later–occurring secondary cell death, could reveal essential interdependencies of cerebellar neurons and should open interesting routes for future research.

Clearance of apoptotic bodies involves microglial phagocytosis

After the treatment with 4OHT for 16 hours on 4 dpf we observed an accumulation of apoptotic bodies from dying or dead PCs. When larvae were analyzed again 24, 48 and 72 hrs later by *in vivo* confocal microscopy, the amount of debris derived from dying PCs was markedly reduced based on the wider spacing of red fluorescent debris and fewer particles in the PC layer (Fig. 2C). This decrease in fluorescent cell debris could be attributed to microglial cells, which are the major phagocytosing cells of the brain. Their number though is low in the cerebellum and increases only slightly - likely because of continued brain growth - from 4 dpf to 5 dpf to about one microglial cell per cerebellar hemisphere (Fig. 5D see number of microglia in EtOH and 4OHT control specimens). Microglia are involved in developmental apoptosis in the larval zebrafish brain (Cole and Ross, 2001), which still

occurs in the optic tectum on 3 dpf, while it has ceased in the cerebellum (Peri and Nüsslein-Volhard, 2008; Sieger and Peri, 2013; Svahn et al., 2013). To address the potential involvement of microglia in the clearance of apoptotic debris, we induced the ablation of PCs on 4 dpf in PC- ATTAC™ larvae in the *Tg*(*pU.1:gal4-uas:egfp*)-background, where microglia are highlighted by their expression of EGFP (Fig. 5) (Peri and Nüsslein-Volhard, 2008).

Strikingly the number of microglia in the cerebellum significantly increased in response to PC ablation (Fig. 5B, D, 2,82 microglia per hemisphere, n=28 hemispheres) alongside with a change in their morphology from ramified to ameboid (Fig. 5E, 66.9% of microglia compared to 20.0% in EtOH control specimens) containing several vacuoles indicating their activation and their involvement in engulfing and phagocytosing PC debris. Indeed, EGFP-expressing cerebellar microglia with internalized red fluorescent PC debris could be observed by confocal microscopy sectioning (Fig. 5B). Such an increase in microglia number or change in microglia morphology could neither be observed in EtOH controls (Fig. 5A, D, F 0.79 microglia per hemisphere, n=14 hemispheres) or *Tg*(*pU.1:gal4-uas:egfp*) transgenic larvae treated with 4OHT (Fig. 5C, D 0.5 microglia per hemisphere, n=11 hemispheres). Furthermore, microglia numbers were not significantly affected in the nearby optic tectum (Fig. 5E, 7.6 (4OHT/PC-ATTAC™), 6.9 (EtOH/PC-ATTAC™), 7.0 (4OHT/*pU.1:gal4-uas:egfp)* microglia, with 28, 14 and 11 analyzed tectal areas respectively) neither increasing nor decreasing to support microglia in the cerebellum, which is consistent with the finding that microglia avoid to cross tissue boundaries such as the MHB or the midline (Sieger et al., 2012). This indicates that the induced acute PC apoptosis results in the increase of microglia in the cerebellum to remove PC debris. Probably because the number of microglia of about 3 per cerebellar hemisphere is still rather low, complete removal of debris lasts for about 2-3 days (Fig. 2C). Recent elegant studies have demonstrated that upon cell death in the developing brain invasion of macrophages into the zebrafish larval brain occurs where these macrophages differentiate into microglia (van Ham et al., 2014; Casano et al., 2016). These findings provide an explanation for the increase in microglia numbers that we observed in the cerebellum of 4OHT treated PC- ATTAC™ larvae.

Discussion

Using cell type specific expression of a Tamoxifen-indcubible initiator Caspase8 we have established a stable transgenic strain named PC- ATTAC™ as a genetic model for cerebellar Purkinje cell ablation. The coexpression of a fluorescent protein with Caspase8ER^{T2} helps not only to monitor and verify the course and extent of apoptotic PC death, but also allows for observing cell interactions such as the activity of microglia with dying PCs.

Our data demonstrate the engagement of microglia in the uptake and probably removal of dying or dead PCs after caspase-mediated apoptotic cell ablation in PC- ATTAC™ zebrafish larvae similar to the normal role of microglia during developmental apoptosis. This fast response of microglia may indeed reflect the young age of the larvae, since in adult brains of other non-mammalian vertebrates a detectable increase in the numbers of microglia at the site of neuronal ablation has been shown to take up to three days, after which their increased numbers remain stable at the site of lesion for several weeks (Kirkham et al., 2011). Our findings could reflect the importance of a microglia response to cell ablation in the brain for subsequent restructuring and regeneration processes. Importantly this endogenous neuroinflammatory response should be left unaltered by 4OHT as this compound does not significantly influence innate immunity thereby providing the chance to reveal the significance of neuroinflammation in mediating the brain's response to the acute loss of specific neuronal populations. In addition, ablation and removal of nearly all PCs will not allow plasticity to compensate for a loss of cerebellum function but requires regeneration for cerebellum recovery. Thus after removal of Tamoxifen, fluorescent protein expression will make the dynamics of potential PC regeneration accessible by bio-imaging approaches with membrane-targeted fluorescence facilitating the observation of regenerative axon and dendrite outgrowth.

Based on our results in transient transgenics other cell types should be equally accessible for the generation of ATTAC™ -zebrafish with Tamoxifen-inducible apoptosis. The time course of differentation specific for each cell type has to be taken into account though. If ablation is induced too early, progenitor cells not expressing the inducible caspase yet, may

escape the induction of apoptosis. To distinguish between such late-differentiating progenitor cells and non-ablated mature cells the use of fluorescent proteins with time-dependent change in the colour of fluorescence emission (so-called timer fluorescent proteins) could be used as co-expressed reporters (Terskikh et al., 2000; Tsuboi et al., 2010). While mature cells that escaped apoptosis will appear in the late-emission state of the fluorescent timer protein, cells that escaped ablation for the sake of their late birth will just start to express the fluorescent protein and will thus appear in the early-emission state. Because ligand-induced activity is also dependent on the cellular expression level of Caspase8ER^{T2}, which is determined by the promoter strength that drives such expression, the optimal conditions for maximal ablation will have to be tested empirically when implementing new promoter/enhancer elements into ATTAC™ -constructs. We recommend starting with a Tamoxifen-concentration of $5x10^{-6}$M diluted in EtOH at a maximum concentration of 0.5% EtOH and treatment over night.

Transgenic cell type specific ATTAC™ -zebrafish complement the existing NTR-mediated inducible cell ablation method. For one the ATTAC™ approach may broaden the range of cell types that could be targeted by inducible cell death. In addition, unlike metronidazole Tamoxifen neither exerts antibiotic nor prominent anti-inflammatory activity. Thus when cell ablation and its consequences are to be studied in the context of a naturally occuring inflammatory responses such as the behaivors of microglia, macrophages or neutrophils and their contribution to post-ablation processes, ATTAC™ -zebrafish may serve as an informative tool.

In summary, the choice of the ablation approach – mechanically, genetically, chemically or light-induced – will influence subsequent events such as regeneration or remodelling of neuronal connections, and these issues have to be evaluated by the investigator. Here we introduce a useful supplement to the steadily growing genetic zebrafish toolbox in form of a fast, efficient and inducible cell ablation method thereby enlarging the technical possibilities to choose from.

MATERIALS & METHODS

Animal husbandry

Zebrafish were maintained under 14 hours light/ 10 hours dark cycles at 28°C. Juvenile and adult fish were treated according to the Declaration of Helsinki for the care and use of animals and in accordance with legal regulations (EU-Directive 201_63). Phenylthiourea (PTU, 0.15 mM) to reduce pigmentation was only used where indicated. In addition, established transgenic lines expressing KalTA4 in the ventral neural tube (hzm9; Babaryka et al., 2009), in rhombomere 3 and 5 (hzm6Et) and in skeletal muscles (hzm8Et; Distel et al., 2009) were used as well as Tg(*ca8-ADV.E1b:TagRFP*)bz4Tg also named PC-FyntagRFP-T as control (Matsui et al., 2014).

Cloning of constructs

A pB-Tol2 construct was used as backbone into which a PC-specific enhancer (Matsui et al., 2014) /CMV basal promoter was inserted followed by FyntagRFP - a membrane targeted red fluorescent protein tagRFP - fused to a T2A-peptide, myrCasp8ER^{T2} (Chu et al., 2008), the chicken **β**-globin intron and SV40 polyA sequences (GIpA) to result in the final construct „pBS_Tol2-*SalI*-PC:-*EcoRI*:FP-*SpeI*-T2A-myrCasp8ER^{T2}-*XbaI*-GIpA-*NotI*“ (Fig. 1B) (#2498 in Köster lab plasmid database). Note that the cell-type specific promoter and the FP can be exchanged using unique SalI/EcoRI- and EcoRI/SpeI sites respectively.
For transient transgenic assays transgene cassettes encoding FyntagRFP-T, FyntagRFP-T-T2A-CaspaseER^{T2}, or FynVenus-T2A-CaspaseER^{T2} flanked by 5xUAS-E1b and globin intron-SV40 polyA (Distel et al., PNAS, 2009), were cloned into pDon122 allowing for Tol1 mediated-genome integrations (Koga et al., 2008).

Generation of transgenic zebrafish

Constructs were injected into fertilized eggs at the one-cell stage of WT embryos together with *Tol2 transposase* mRNA (Kawakami, 2007) and embryos displaying PC-specific fluorescence at 4 dpf were raised to adulthood. Transgene inheritance was followed to the F3 generation. Initially three independent lines were established, two of which displayed

efficient PC-ablation. One of these was subsequently maintained and named Tg(*ca8:FMA-TagRFP-2A-casp8ERT2*)^{bz11Tg} or PC- ATTAC™.

Cell ablation

For transient transgenic cell ablations pDon122 Gal4-dependent Caspase8ER^{T2} constructs were injected into Gal4 expression lines together with *tol1* mRNA (25ng/µl each) at the one cell stage. Dechorionated (1mg/ml pronase) 24 hpf embryos were treated with either 0.5% EtOH or 5µM 4-hydroxy-tamoxifen (4OHT, Sigma Aldrich) or 3µM Staurosporine (Sigma Aldrich) in 30% Danieau medium. Apoptotic cells were detected by staining for 1 h in 10µg/ml acridine orange (Sigma Aldrich)/30% Danieau and observed under a confocal microscope.

For stable transgenic ablation in 24 well plates up to 6 heterozygous PC- ATTAC™ larvae were kept in 1 ml 30% Danieau/PTU supplemented with 4OHT at a final concentration of $5x10^{-6}$M from stock (10^{-3}M in EtOH) that was stored at -20°C protected from light. Incubation was performed at 28°C in the dark for up to 16hrs followed by transfer into fresh 30% Danieau/PTU. Each experiment was paralleled by controls with embryos treated in 0.5% EtOH.

Imaging

Larvae were anesthesized in 0.04mg/ml tricaine (MS-222, Sigma) and embedded in 1% ultra low melting agarose dissolved in 30% Danieau/PTU. Images were recorded with a confocal microscope (LSM510, Zeiss and SP8 Leica) using a 40xApochromat water immersion objective (NA 1.2) and subsequently processed with respective microscope software, ImageJ (NIH), Photoshop and Illustrator (Adobe).

Purkinje cells were counted manually from confocal z-stacks throughout the complete right cerebellar hemisphere. Microglia were counted in the right cerebellar hemisphere and compared to a part of the optic tectum of similar size (55x80µm).

RT-PCR

After treatment with 4OHT or EtOH total RNA was extracted from pools of 5 embryo heads using peqGOLD (Peqlab). 2µg of total RNA was reverse transcribed with 50µM oligo(dT)

primers, 2.5mM dNTPs and 10U AMV reverse transcriptase (Promega) for 1h at 42°C. RT-PCR experiments (n=3) were performed with GoTaq (Promega). β-actin mRNA expression was used to normalize the expression of RFP. The following primers were used. β-actin fp 5'-TCTGTTGGCTTTGGGATTC-3'; β-actin rp: 5'-TCTGTTGGCTTTGGGATTC-3'; tagRFP fp: 5'-ATGGTGTCTAAGGGCGAAGAGCTGAT-3'; tagRFP rf:5'-TCAATTAAGTTTGTGCCCCAGTTTGC-3'.

Expression analysis

For whole mount *in situ* hybridization larvae were fixed in 4%PFA/PBS overnight and processed according to an established protocol (Volkmann et al., 2010).

To detect Venus cleaved Caspase3 by immunohistochemistry embryos at 1dpf were fixed in 4%PFA/PBS 6hrs after treatment with EtOH or 4OHT. Larvae at 4 or 5dpf were fixed after 4OHT treatment in 4%PFA/PBS for 3hrs or overnight. For sectioning, brains from adults older than 15 months were fixed with 4%PFA/PBS overnight at 4°C followed by cryoprotection in 20%sucrose/PBS. After embedding in Tissue-Tek (O.C.T.) cryotome sections were prepared at a thickness of 20 µm.

The following primary antibodies were used: polyclonal rabbit IgG α-cleaved Caspase3 (1:2000, Abcam, ab13847), polyclonal chicken IgY α-GFP (1:1000, Aves labs, GFP-1020), monoclonal mouse α-ZebrinII (1:300, kind gift from Richard Hawkes), polyclonal rabbit IgG α-tRFP (1:2000, Evrogen, AB233), monoclonal rabbit α-Caspase8 IgG (EPR17366) (1:2000, Abcam, ab181580). The following secondary antibodies were used: donkey α-chick IgY FITC (1:1000, Jackson Immunoresearch, 703-545-155), donkey α-rabbit IgG Alexa647 (1:1000, Thermofisher Scientific, A-31573), donkey α-rabbit IgG Alexa546 (1:500, Thermofisher Scientific, A-10040) and donkey α-mouse IgG Alexa488 (1:500, Thermofisher Scientific, A-21202).

Western blot analysis

For western blot analysis dissected adult cerebellar tissues were homogenized with a hand pestle in 80µl of NP40 lysis buffer (20mMTris-HCl, 180mM NaCl, 1mM EDTA, 0.5% NP40), and further lysed by sonication (Bioruptor UCD-300 TM ultrasound sonicator, Diagenode).

12.5µl of the cleared lysate per lane was subjected to 10% SDS polyacrylamide gel electrophoresis, and transferred to a PVDF membrane (Membrane Roti®-Fluoro PVDF, Carl Roth). The following primary antibodies were used: polyclonal rabbit α-tRFP antibody (1:2000, Evrogen, AB233) and monoclonal rabbit α-Caspase8 (EPR17366) (1:1000, Abcam, ab181580). As secondary antibody an HRP-conjugated goat α-rabbit IgG antibody (1:10,000, Jackson ImmunoResearch, 111-035-144) was used and visualized by chemiluminescence (SERVALight Eos CL HRP WB Substrate Kit, Serva Electrophoresis).

ACKNOWLEDGEMENTS

We thank Enrico Kühn for assistance with microinjections, Christiane Lach for the accomplishment of EtOH-toxicity studies and all members of the lab for helpful discussions.

Funding

The work of RWK was funded by the Federal State of Lower Saxony, Niedersächsisches Vorab (VWZN2889). The work of WW was supported by the German Science Foundation Collaborative Research Centre (CRC) 870 and the Bundesministerium für Bildung und Forschung (BMBF) grant 'TAL-*Cut*-Technology' (03V0261).

COMPETING INTERESTS

The authors declare no competing interests.

AUTHOR CONTRIBUTIONS

TW, KN, BW, KMB and RWK designed the experiments and analyzed data, TW, KN, BW, KMB performed experiments, all authors wrote the manuscript.

REFERENCES

Babaryka, A., Kühn, E., Köster, R. W. (2009). In vivo synthesis of meganuclease results in efficient transgenesis in zebrafish. *J Fish Biol* **74**: 452-457.

Bae, Y. K., Kani, S., Shimizu, T., Tanabe, K., Nojima, H., Kimura, Y., Higashijima, S. and Hibi, M. (2009). Anatomy of zebrafish cerebellum and screen for mutations affecting its development. *Dev Biol* **330**, 406-426.

Bardet, P. L., Horard, B., Robinson-Rechavi, M., Laudet, V. and Vanacker, J. M. (2002). Characterization of oestrogen receptors in zebrafish (Danio rerio). *J Mol Endocrinol* **28**, 153-163.

Biechl, D., Dorigo, A., Köster, R. W., Grothe, B., Wullimann, M. F. (2016): Eppur Si Muove: Evidence for an external granular layer and possibly transit amplification in the teleostean cerebellum. *Front Neuroanat* **10**, 49.

Bridgewater, J. A., Knox, R. J., Pitts, J. D., Collins, M. K. and Springer, C. J. (1997). The bystander effect of the nitroreductase/CB1954 enzyme/prodrug system is due to a cell-permeable metabolite. *Hum Gene Ther* **8**, 709-717.

Bulina, M. E., Lukyanov, K. A., Britanova, O. V., Onichtchouk, D., Lukyanov, S. and Chudakov, D. M. (2006). Chromophore-assisted light inactivation (CALI) using the phototoxic fluorescent protein KillerRed. *Nat Protoc* **1**, 947-953.

Casano, A. M., Albert, M., Peri, F. (2016). Developmental apoptosis mediates entry and positioning of microglia in the zebrafish brain. *Cell Reports* **16**, 1-10.

Chen, C. F., Chu, C. Y., Chen, T. H., Lee, S. J., Shen, C. N. and Hsiao, C. D. (2011). Establishment of a transgenic zebrafish line for superficial skin ablation and functional validation of apoptosis modulators in vivo. *PLoS One* **6**, e20654.

Chu, Y., Senghaas, N., Köster, R. W., Wurst, W. and Kühn, R. (2008). Novel caspase-suicide proteins for Tamoxifen-inducible apoptosis. *Genesis* **46**, 530-536.

Cole, L. K. and Ross, L. S. (2001). Apoptosis in the developing zebrafish embryo. *Dev Biol* **240**, 123-142.

Cui, W., Gusterson, B. and Clark, A. J. (1999). Nitroreductase-mediated cell ablation is very rapid and mediated by a p53-independent apoptotic pathway. *Gene Ther* **6**, 764-770.

Curado, S., Anderson, R. M., Jungblut, B., Mumm, J., Schroeter, E. and Stainier, D. Y. (2007). Conditional targeted cell ablation in zebrafish: a new tool for regeneration studies. *Dev Dyn* **236**, 1025-1035.

Davison, J. M., Akitake, C. M., Goll, M. G., Rhee, J. M., Gosse, N., Baier, H., Halpern, M. E., Leach, S. D. and Parsons, M. J. (2007). Transactivation from Gal4-VP16 transgenic insertions for tissue-specific cell labeling and ablation in zebrafish. *Dev Biol* **304**, 811-824.

de Anda, F. C., Meletis, K., Ge, X., Rei, D. and Tsai, L. H. (2010). Centrosome motility is essential for initial axon formation in the neocortex. *The Journal of neuroscience : the official journal of the Society for Neuroscience* **30**, 10391-10406.

Distel M., Wullimann, M. F., Köster, R. W. (2009). Optimized Gal4-genetics for permanent gene expression mapping in zebrafish. *PNAS* **106**, 13365-13370.

Djeha, H. A., Todryk, S. M., Pelech, S., Wrighton, C. J., Irvine, A. S., Mountain, A. and Lipinski, K. S. (2005). Antitumor immune responses mediated by adenoviral GDEPT using nitroreductase/CB1954 is enhanced by high-level coexpression of heat shock protein 70. *Cancer Gene Ther* **12**, 560-571.

Fernandez-Gonzalez, A., La Spada, A. R., Treadaway, J., Higdon, J. C., Harris, B. S., Sidman, R. L., Morgan, J. I. and Zuo, J. (2002). Purkinje cell degeneration (pcd) phenotypes caused by mutations in the axotomy-induced gene, Nna1. *Science* **295**, 1904-1906.

Goetz, M. P., Kamal, A. and Ames, M. M. (2008). Tamoxifen pharmacogenomics: the role of CYP2D6 as a predictor of drug response. *Clin Pharmacol Ther* **83**, 160-166.

Hamling, K. R., Tobias, Z. J. C., Weissman, T. A. (2015). Mapping the development of cerebellar Purkinje cells in zebrafish. *Dev Neurobiol* **75**, 1174-1188.

Hans, S., Kaslin, J., Freudenreich, D. and Brand, M. (2009). Temporally-controlled site-specific recombination in zebrafish. *PLoS One* **4**, e4640.

Hibi, M. and Shimizu, T. (2012). Development of the cerebellum and cerebellar neural circuits. *Dev Neurobiol* **72**, 282-301.

Kameda, H., Furuta, T., Matsuda, W., Ohira, K., Nakamura, K., Hioki, H. and Kaneko, T. (2008). Targeting green fluorescent protein to dendritic membrane in central neurons. *Neurosci Res* **61**, 79-91.

Kaslin, J., Kroehne, V., Benato, F., Argenton, F., Brand M. (2013). Development and specification of cerebellar stem and progenitor cells in zebrafish: from embryo to adult. *Neural Dev* **8**: 9.

Kawakami, K. (2007). Tol2: a versatile gene transfer vector in vertebrates. *Genome Biol* **8 Suppl 1**, S7.

Kim, J. H., Lee, S. R., Li, L. H., Park, H. J., Park, J. H., Lee, K. Y., Kim, M. K., Shin, B. A. and Choi, S. Y. (2011). High cleavage efficiency of a 2A peptide derived from porcine teschovirus-1 in human cell lines, zebrafish and mice. *PLoS One* **6**, e18556.

Kirkham, M., Berg, D. A. and Simon, A. (2011). Microglia activation during neuroregeneration in the adult vertebrate brain. *Neurosci Lett* **497**, 11-16.

Koga, A., Cheah, F. S., Hamaguchi, S., Yeo, G. H., Chong, S. S. (2008). Germline transgenesis of zebrafish using the medaka Tol1 transposon system. *Dev Dyn* **237**, 2466-2474.

Korzh, V., Teh, C., Kondrychyn, I., Chudakov, D. M. and Lukyanov, S. (2011). Visualizing compound transgenic zebrafish in development: a tale of green fluorescent protein and KillerRed. *Zebrafish* **8**, 23-29.

Kroehne, V., Freudenreich, D., Hans, S., Kaslin, J. and Brand, M. (2011). Regeneration of the adult zebrafish brain from neurogenic radial glia-type progenitors. *Development* **138**, 4831-4841.

Lannoo, M. J., Ross, L., Maler, L. and Hawkes, R. (1991). Development of the cerebellum and its extracerebellar Purkinje cell projection in teleost fishes as determined by zebrin II immunocytochemistry. *Prog Neurobiol* **37**, 329-363.

Lieschke, G. J. and Currie, P. D. (2007). Animal models of human disease: zebrafish swim into view. *Nat Rev Genet* **8**, 353-367.

Lin, J. W., Biankin, A. V., Horb, M. E., Ghosh, B., Prasad, N. B., Yee, N. S., Pack, M. A. and Leach, S. D. (2004). Differential requirement for ptf1a in endocrine and exocrine lineages of developing zebrafish pancreas. *Dev Biol* **274**, 491-503.

Lipinski, K. S., Pelech, S., Mountain, A., Irvine, A. S., Kraaij, R., Bangma, C. H., Mills, K. H. and Todryk, S. M. (2006). Nitroreductase-based therapy of prostate cancer, enhanced by raising expression of heat shock protein 70, acts through increased anti-tumour immunity. *Cancer Immunol Immunother* **55**, 347-354.

Long, Q., Meng, A., Wang, H., Jessen, J. R., Farrell, M. J. and Lin, S. (1997). GATA-1 expression pattern can be recapitulated in living transgenic zebrafish using GFP reporter gene. *Development* **124**, 4105-4111.

Mathias, J. R., Zhang, Z., Saxena, M. T., Mumm, J. S. (2014). Enhanced cell-specific ablation in zebrafish using a triple mutant of Escherichia coli nitroreductase. *Zebrafish* **11**, 85-97.

Matsui, H., Namikawa, K., Babaryka, A. and Koster, R. W. (2014). Functional regionalization of the teleost cerebellum analyzed in vivo. *Proc Natl Acad Sci U S A* **111**, 11846-11851.

Mosimann, C., Kaufman, C. K., Li, P., Pugach, E. K., Tamplin, O. J. and Zon, L. I. (2011). Ubiquitous transgene expression and Cre-based recombination driven by the ubiquitin promoter in zebrafish. *Development* **138**, 169-177.

Pajvani, U. B., Trujillo, M. E., Combs, T. P., Iyengar, P., Jelicks, L., Roth, K. A., Kitsis, R. N., Scherer, P. E. (2005). Fat apoptosis through targeted activation of caspase 8: a new mouse model of inducible and reversible lipoatrophy. *Nature Medicine* **11**, 797-803.

Park, H. C., Mehta, A., Richardson, J. S. and Appel, B. (2002). olig2 is required for zebrafish primary motor neuron and oligodendrocyte development. *Dev Biol* **248**, 356-368.

Peri, F. and Nüsslein-Volhard, C. (2008). Live imaging of neuronal degradation by microglia reveals a role for v0-ATPase a1 in phagosomal fusion in vivo. *Cell* **133**, 916-927.

Pisharath, H. (2007). Validation of nitroreductase, a prodrug-activating enzyme, mediated cell death in embryonic zebrafish (Danio rerio). *Comp Med* **57**, 241-246.

Sieger, D. and Peri, F. (2013). Animal models for studying microglia: the first, the popular, and the new. *Glia* **61**, 3-9.

Sieger, D., Moritz, C., Ziegenhals, T., Prykhozhij, S. and Peri, F. (2012). Long-range Ca2+ waves transmit brain-damage signals to microglia. *Dev Cell* **22**, 1138-1148.

Svahn, A. J., Graeber, M. B., Ellett, F., Lieschke, G. J., Rinkwitz, S., Bennett, M. R. and Becker, T. S. (2013). Development of ramified microglia from early macrophages in the zebrafish optic tectum. *Dev Neurobiol* **73**, 60-71.

Takemoto, K., Matsuda, T., Sakai, N., Fu, D., Noda, M., Uchiyama, S., Kotera, I., Arai, Y., Horiuchi, M., Fukui, K., Ayabe, T., Inagaki, F., Suzuki, H., Nagai, T. (2013). SuperNova, a monomeric photosensitizing fluorescnet protein for chromophore-assisted light inactivation. *Sci Rep* **3**, 2629.

Teh, C., Chudakov, D. M., Poon, K. L., Mamedov, I. Z., Sek, J. Y., Shidlovsky, K., Lukyanov, S. and Korzh, V. (2010). Optogenetic in vivo cell manipulation in KillerRed-expressing zebrafish transgenics. *BMC Dev Biol* **10**, 110.

Terskikh, A., Fradkov, A., Ermakova, G., Zaraisky, A., Tan, P., Kajava, A: V., Zhao, X., Lukyanov, S., Matz, M., Kim, S., Weissman, I., Siebert, P. (2000). "Fluorescent timer": protein that changes color with time. *Science* **290**, 1585-1588.

Tsuboi, T., Kitaguchi, T., Karasawa, S., Fukuda, M., Miyawaki, A. (2010). Age-dependent preferential dense-core vesicle exocytosis in neuroendocrine cells revealed by newly developed monomeric fluorescent timer protein. *Mol Biol Cell* **21**, 87-94.

van Ham, T. J., Brady, C. A., Kalicharan, R. D., Oosterhof, N., Kuipers, J., Veenstra-Algra, A., Sjollema, K. A., Peterson, R. T:, Kampinga, H. H., Giepmans, B. N. (2014). Intravital correlated micrcoscopy reveals differential macrophage and microglial dynamics during resolution of neuroinflammation. *Dis Model Mech* **7**, 857-869.

Volkmann, K., Rieger, S., Babaryka, A. and Köster, R. W. (2008). The zebrafish cerebellar rhombic lip is spatially patterned in producing granule cell populations of different functional compartments. *Dev Biol* **313**, 167-180.

Volkmann, K., Chen, Y.-Y., Harris, M., Wullimann, M. F., Köster, R. W. (2010). The zebrafish cerebellar upper rhombic lip generates tegmental hindbrain nuclei by long-distance migration in an evolutionary conserved manner. *J Comp Neurol* **518**, 2794-2817.

Weber, T. and Köster, R. (2013). Genetic tools for multicolor imaging in zebrafish larvae. *Methods* **62**, 279-291.

White, D. T. and Mumm, J. S. (2013). The nitroreductase system of inducible targeted ablation facilitates cell-specific regenerative studies in zebrafish. *Methods* **62**, 232-240.

FIGURES

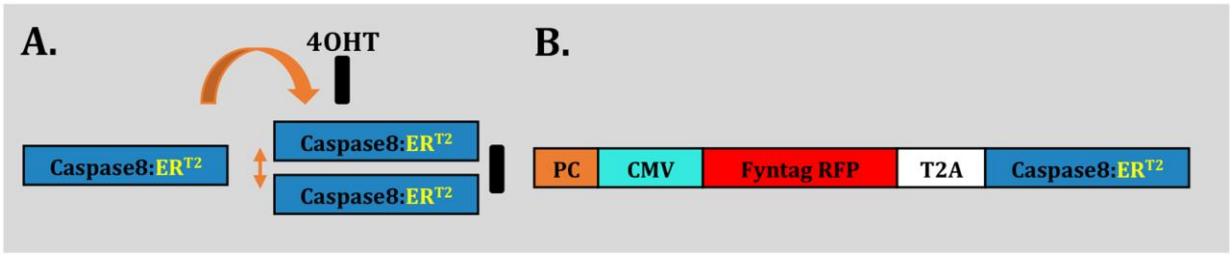

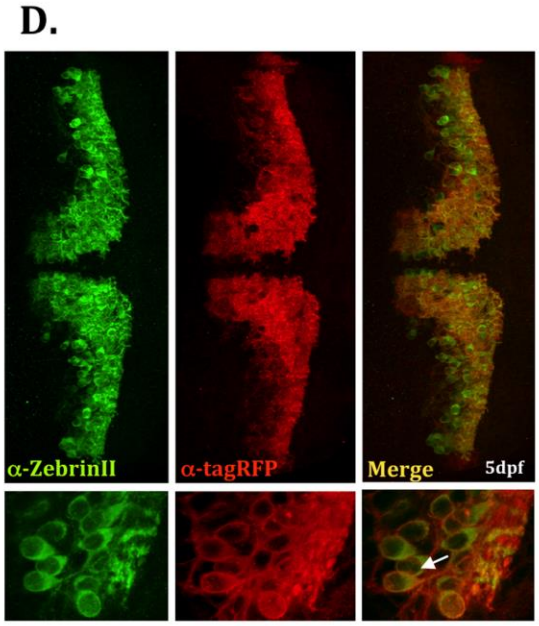

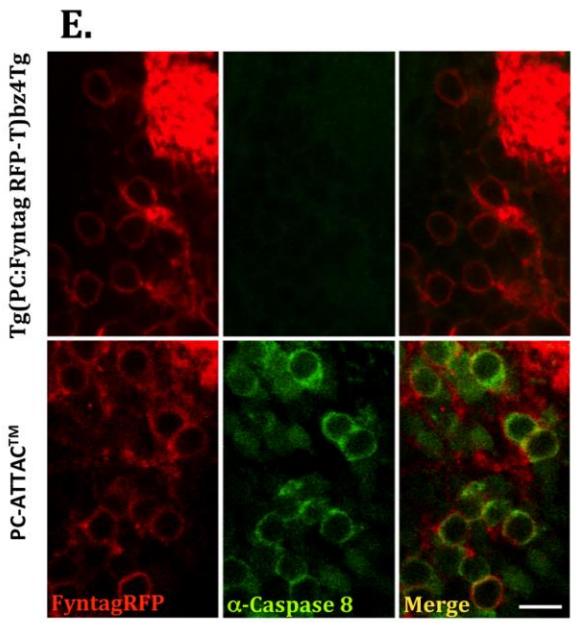

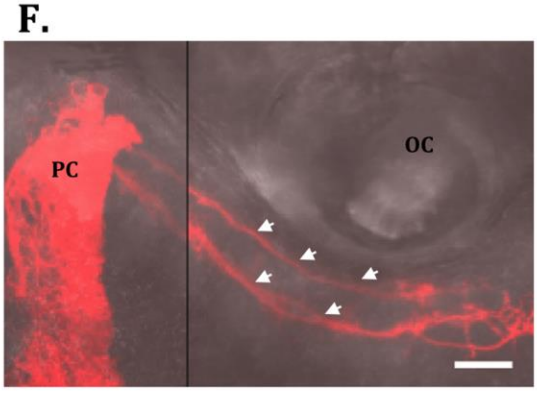

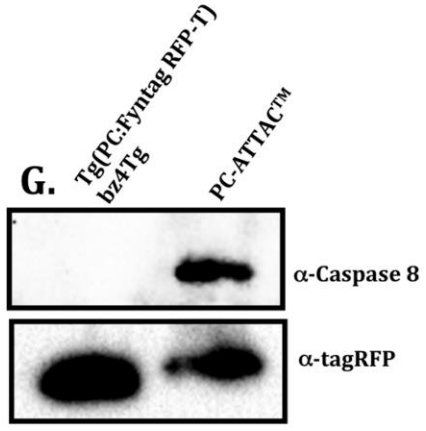

Figure 1: Purkinje cell specific expression of a Tamoxifen-inducible caspase

(A) Schematic diagram of the caspase8 activation: Caspase8 fused to the mutant estrogen receptor ligand binding domain (ER^{T2}) dimerizes upon addition of tamoxifen (4OHT). Subsequent proteolytic self activation of Caspase8 leads to activation of endogenous Caspase3 and cell apoptosis. (B) Construct design for the generation of stable transgenic zebrafish PC-ATTAC™ strain. Membrane bound fluorescent FyntagRFP together with $Caspase8ER^{T2}$ linked by a self-cleaving T2A-peptide is coexpressed under the control of a Purkinje cell-specific regulatory element (PC) from *carbonic anhydrase 8*, which is combined with a CMV basal promoter (CMV) (C) F2-transgenic larvae were analyzed at 5dpf by confocal microscopy to verify transgene encoding FyntagRFP expression exclusively in the cerebellum. (D-E) Purkinje cell (PC) specific expression of the transgene was confirmed by double-immunostainings against (D) FyntagRFP (red) and ZebrinII (green) and (E) Caspase8 (green, combined with FyntagRFP fluorescence) respectively, demonstrating that $Caspase8ER^{T2}$ expression is confined to FyntagRFP-fluorescent ZebrinII expressing PCs. (F) Due to membrane-targeting of FyntagRFP axons, somata and dendrites of PCs, including the long axonal projections forming the cerebello-octavolateralis tract to vestibular nuclei (white arrowheads) could be monitored. (G) Concomitant $Caspase8ER^{T2}$ and FyntagRFP-T or FyntagRFP expression was verfied by Western blot analysis. FyntagRFP-T (bz4Tg, Matsui et al., 2014) alone was used as a control. Abbr.: PC Purkinje cell, oc: otic vesicle.

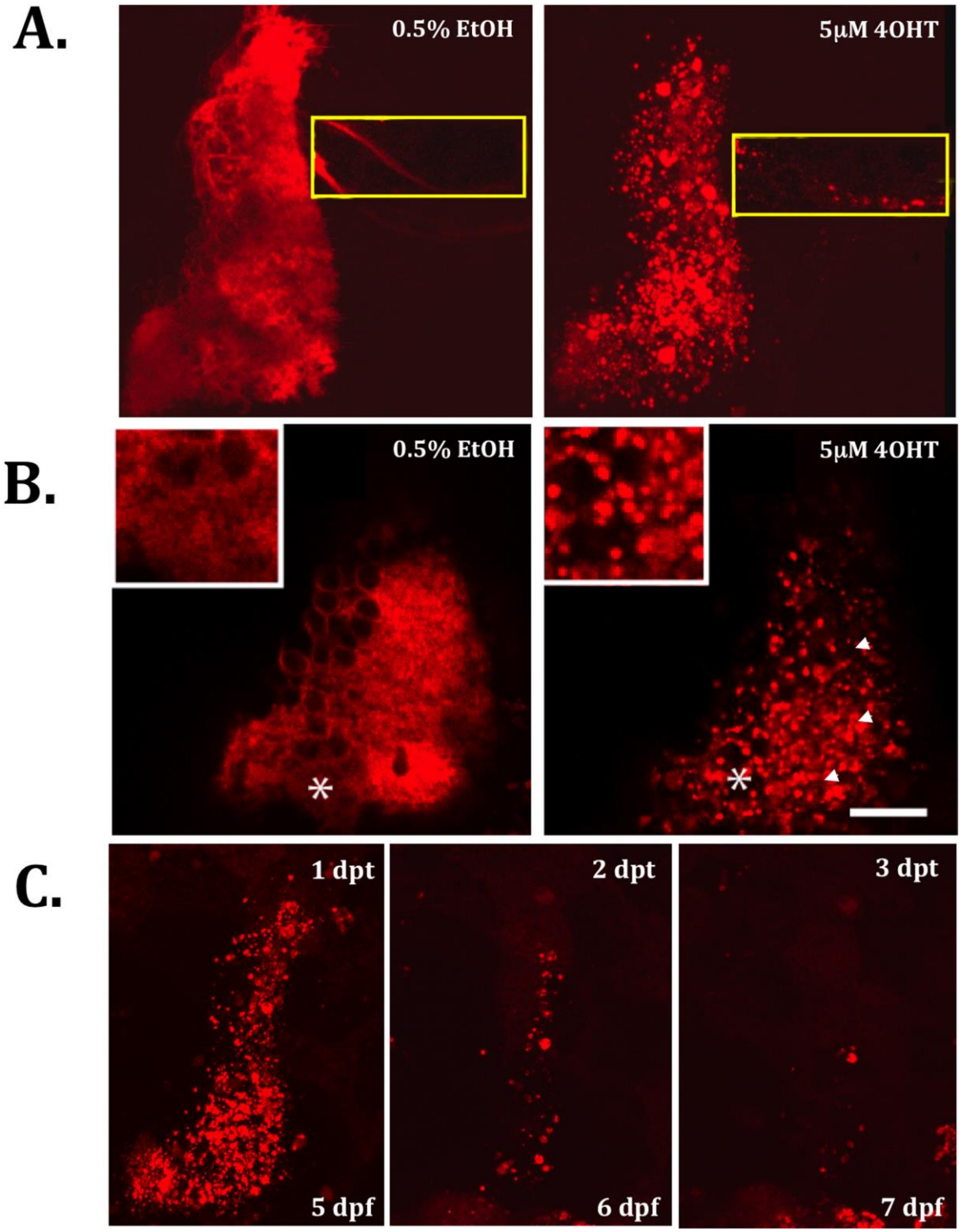

Figure 2: Tamoxifen-induced PC-death in PC-ATTAC™ fish

(A-B) Incubation of 4dpf PC-ATTAC™ embryos (n=6) in 4OHT ($5x10^{-6}$M) for 16h induces cell death of PCs in larvae at 5dpf compared to controls treated with 0.5% EtOH. Cell

ablation was visible by massive PC debris (white arrowheads in B). The extensive dendritic layer was completely disrupted (the star marks the region of the inset in B) and the projections of the cerebello-octavolateralis were fragmented (yellow square in A). (C) PC ablated larvae, re-analyzed 24, 48, and 72h after tamoxifen treatment, show decreasing amounts of red fluorescent PC debris and a lack of fast PC recovery. Scale bars: 20μm; dpt=days post treatment.

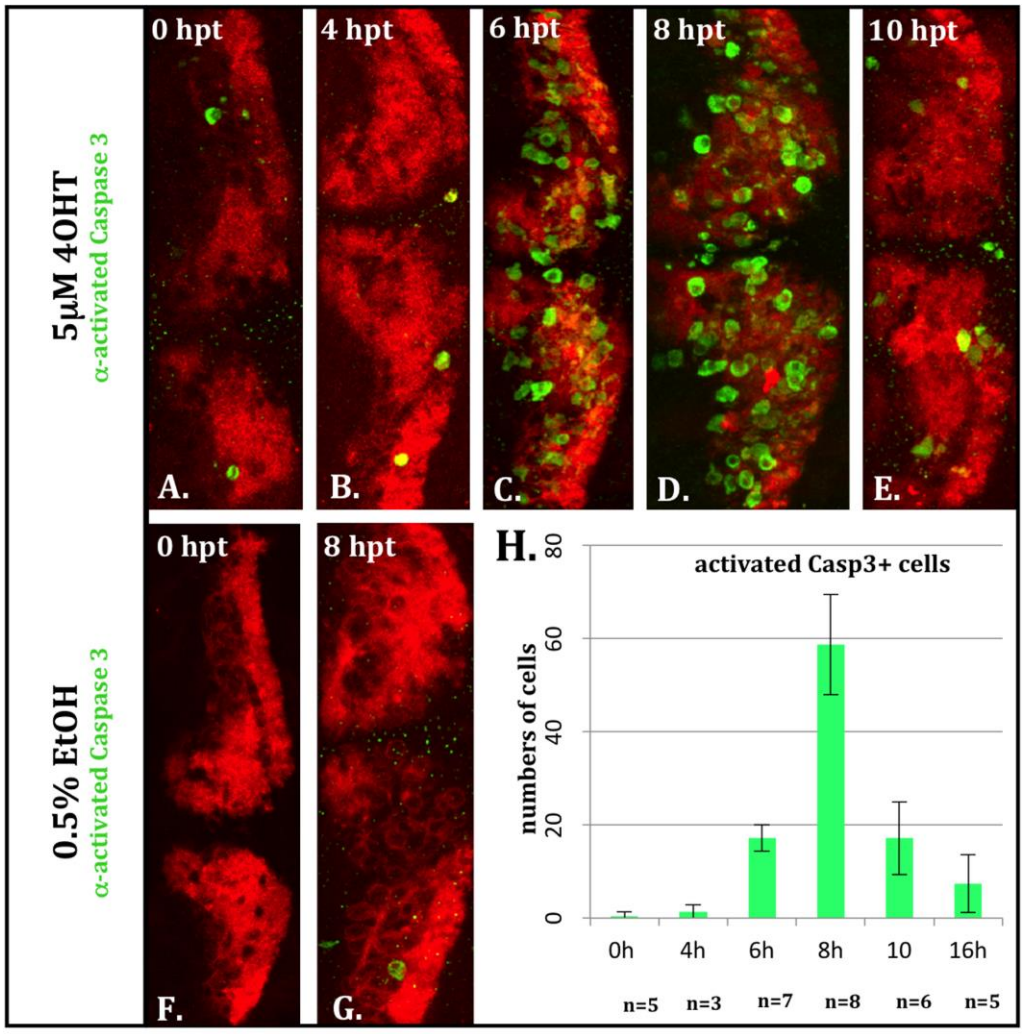

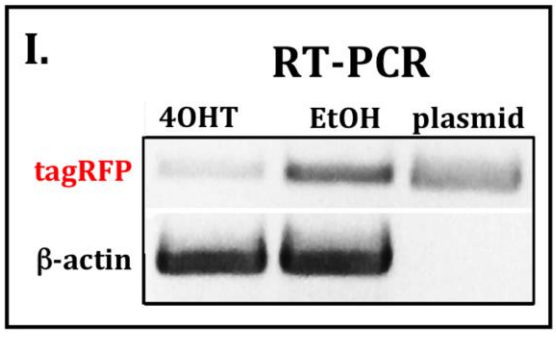

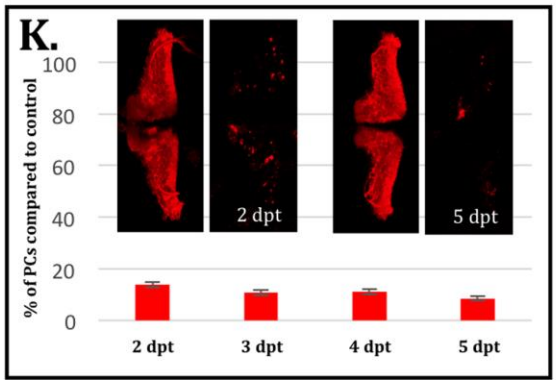

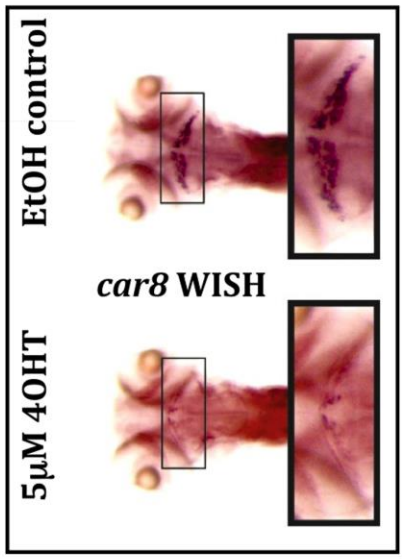

Figure 3: Time course of apoptosis in PC-ATTAC™ larvae

(A-G) Whole mounts of 5dpf transgenic PC-ATTAC™ embryos were stained with an antibody against activated Caspase3 (green) after the treatment at 4dpf with $5x10^{-6}$M 4OHT (A=0h; B=4h; C=6h; D=8h; E=10h) or 5% EtOH (F=0h; G=8h). (H) Significant elevation of apoptosis could be observed after 6 hours peaking after 8 hours of 4OHT treatment based on PC counts at 4dpf. (I-K) To score the extent of PC ablation over time we performed 4OHT treatments with 4dpf heterozygous larvae for 16 hours (compared to 0.5% EtOH controls) and analyzed the cell death 24hours later. (I) RT-PCR revealed a strong reduction of *fyntagRFP* mRNA for 4OHT treated larvae in contrast to EtOH controls with ***β****-actin* used as ubiquitously expressed control gene. (J) While mRNA *in situ* hybridization (n=5) against *carbonic anhydrase 8* (*car8*) was prominent in the cerebellum in control larvae, virtually no *car8* expression was visible in PC-ablated specimens (black squares). (K) Counting of PCs 2 and 5 days post treatment (dpt) revealed a 90% reduction of Purkinje cells compared to EtOH controls (K). hpt=hours post treatment.

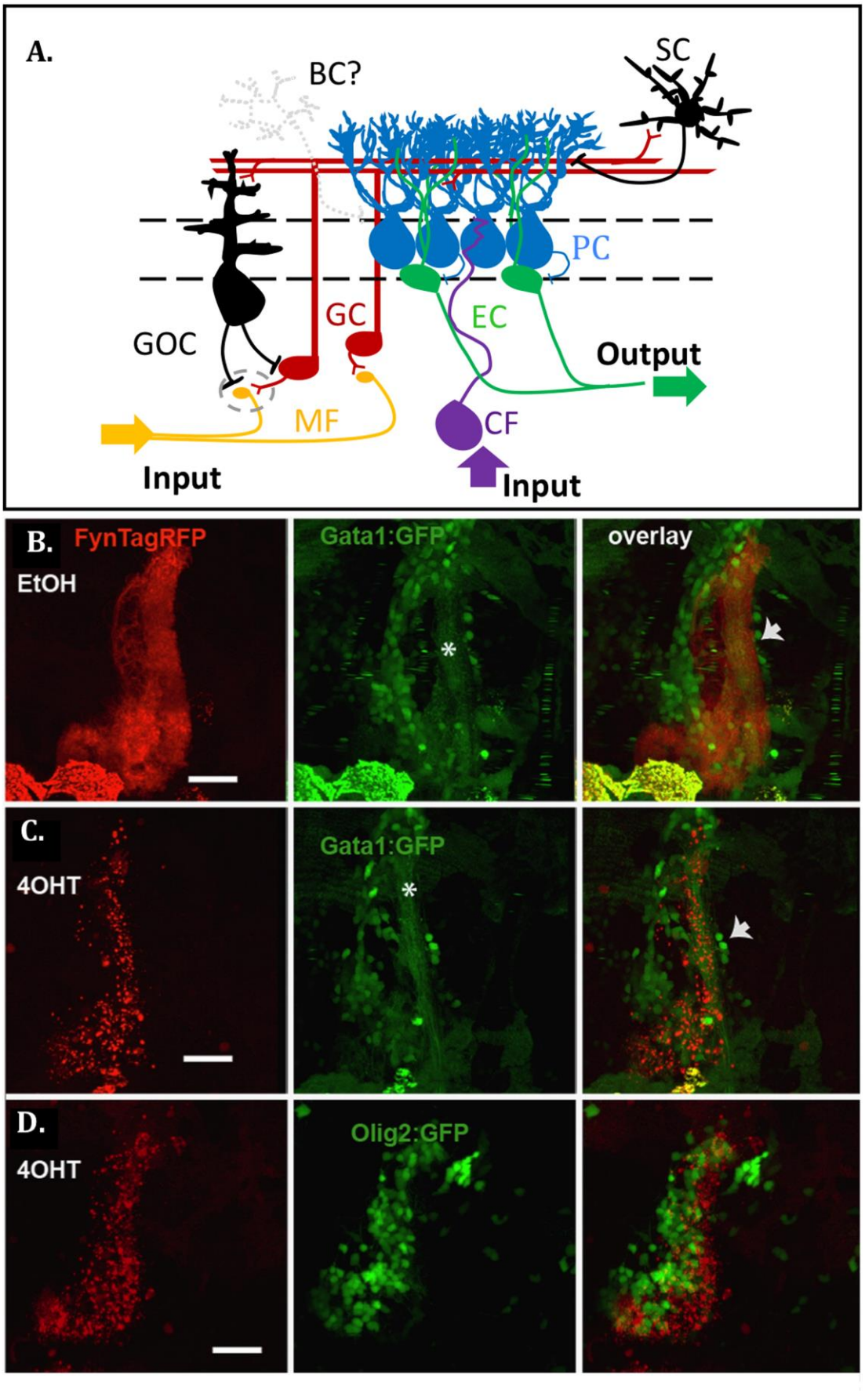

Figure 4: Caspase8ER^{T2}-mediated apoptosis elicits no acute adverse effects on granule and eurydendroid cells.

(A) Schematic presentation of zebrafish cerebellar neurons and circuits. (B-D) Heteorzygous PC- ATTAC^{TM} fish were crossed with carriers of the Tg(*gata1*:*egfp*) strain marking granule cells by green fluorescence (B-C) or with Tg(*olig2*:*egfp*) carriers displaying green fluorescent eurydendroid cells (D). Double transgenic 4dpf larvae were treated with EtOH (B) or 4OHT (C and D) respectively for 16hrs to induce PC ablation followed by confocal microscopy image recording. (C) *gata1:egfp* expressing GCs, somata (arrows) and their axonal projections – the parallel fibers (asterisk) - showed no signs of cell death in contrast to fragmented PCs after 4OHT treatment. (D) The same was true for *olig2:egfp* expressing eurydendroid cells. Scale bars: 20μm. Abbr.: BC=basket cell; EC=eurydendroid cell; CF=climbing fiber; GC=granule cell; GOC=Golgi cell; MF=mossy fiber; PC=Purkinje cell; SC=stellate cell.

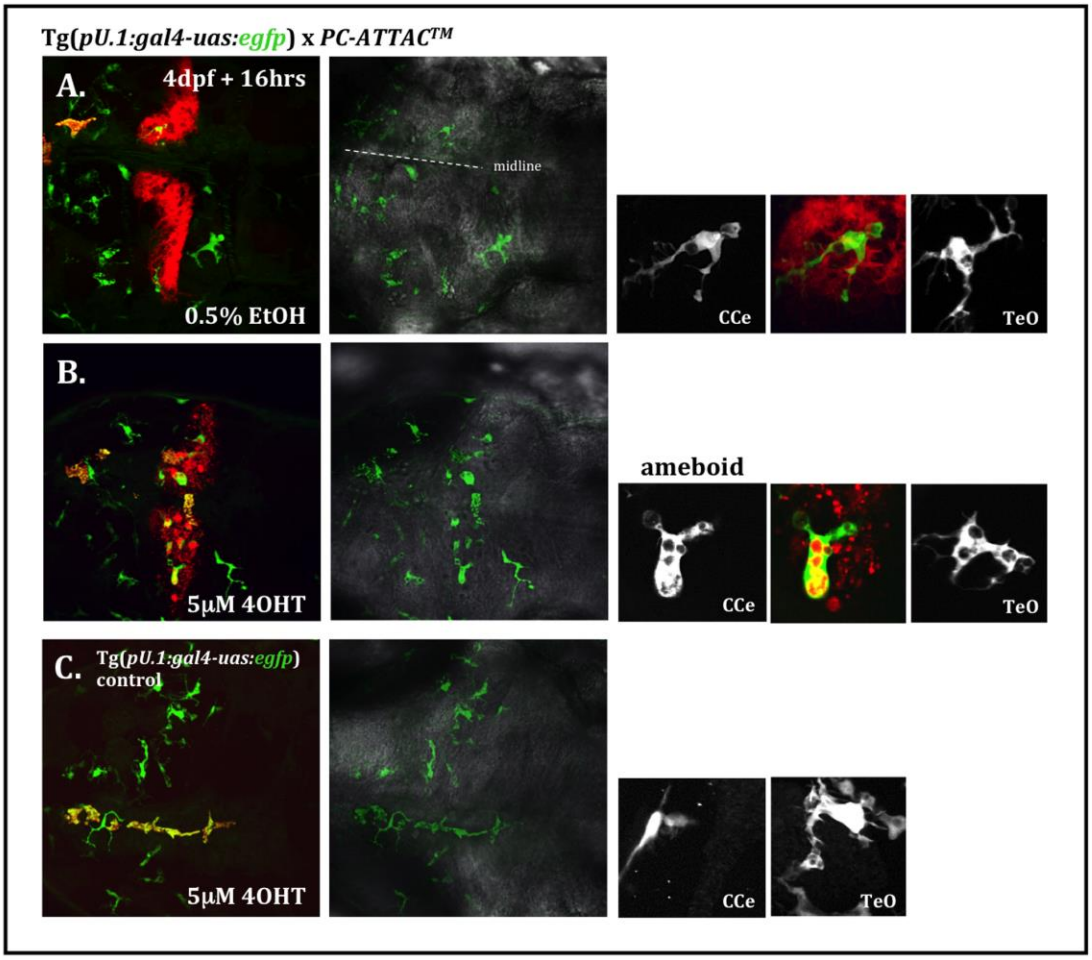

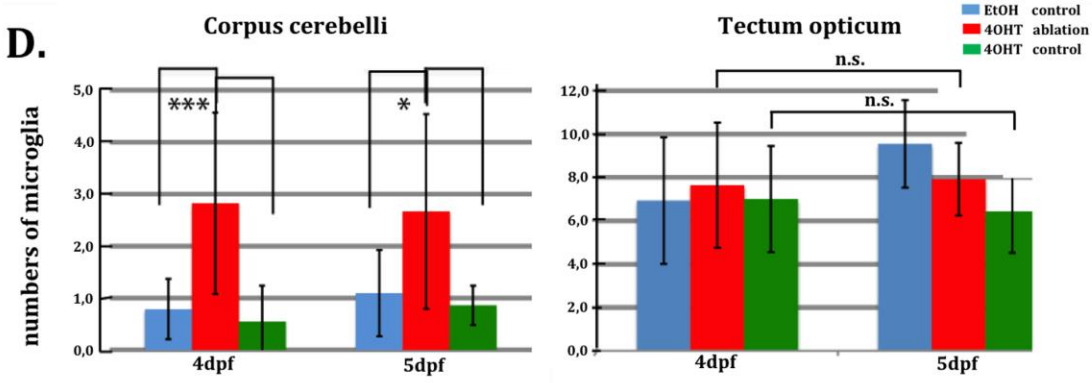

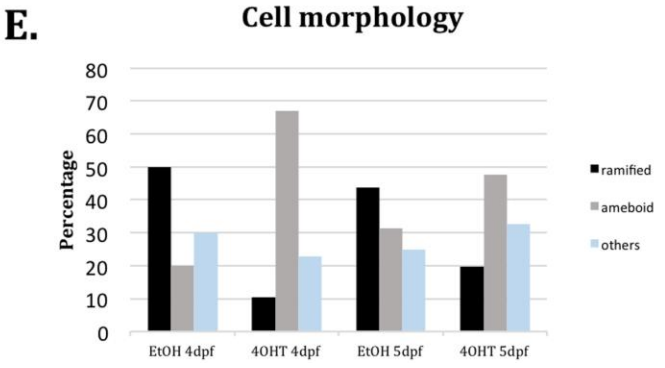

Figure 5: Phagocytosis of apoptotic bodies by microglia.

(A-C) Double transgenic PC- ATTAC™/Tg(*pU.1:gal4-uas:egfp*) larvae with green fluorescent microglial cells in the zebrafish brain. Subjection to PC-ablation (16hrs of 4OHT treatment) caused an increase in numbers of microglial cells specifically in the cerebellum (B, D) accompanied by microglial activation based on ramified to ameboid morphology changes (E). (C) 4OHT treatment of Tg(*pU.1:gal4-uas:egfp*) control larvae had no effect on microglial cells. Abbr.: CCe=corpus cerebelli; TeO=tectum opticum.

Supplementary data – Figures

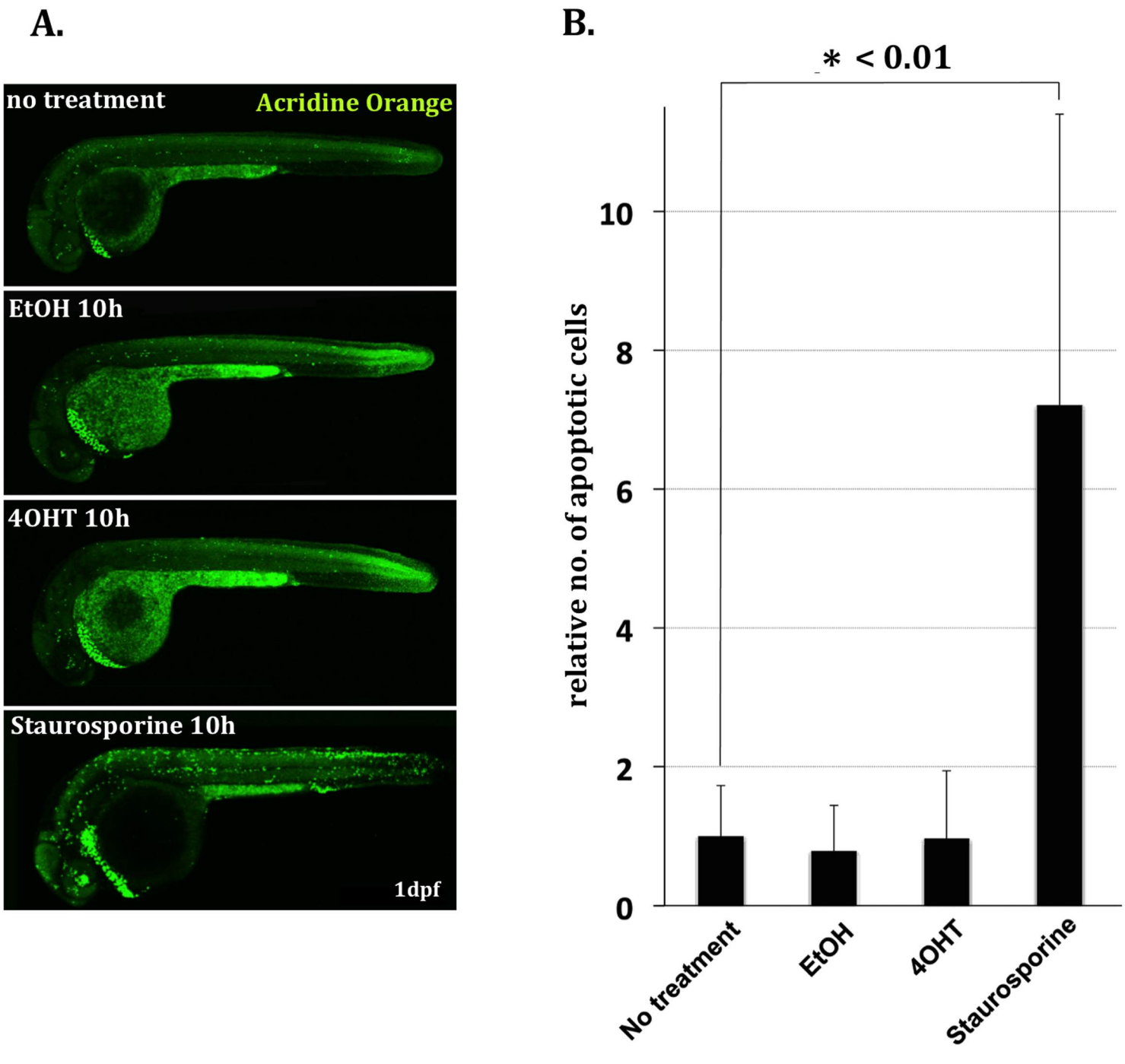

Figure S1: Apoptosis induction by EtOH and 4OHT treatment in zebrafish larvae. (A) Treatments (0.5% EtOH, 5μM 4OHT, 3μM Staurosporine, or non-treatment) were started using wild type zebrafish embryos at 24hpf followed by apoptotic cell detection with acridine orange staining 10hrs later. Whereas Staurosporine treatment induced significant numbers of apoptotic cells, both EtOH- and 4OHT-treated embryos showed similar signals to those obtained in non-treated specimens. (B) Each bar in the graph indicates the relative number of acridine orange positive dying cells throughout the spinal cord region in relation to apoptotic cells in untreated embryos. Counting of the number of apoptotic cells was performed using confocal z-stack images of the spinal cord from 5 independent embryos in each group. * <0.01: p value is lower than 0.01 by Student´s t-test.

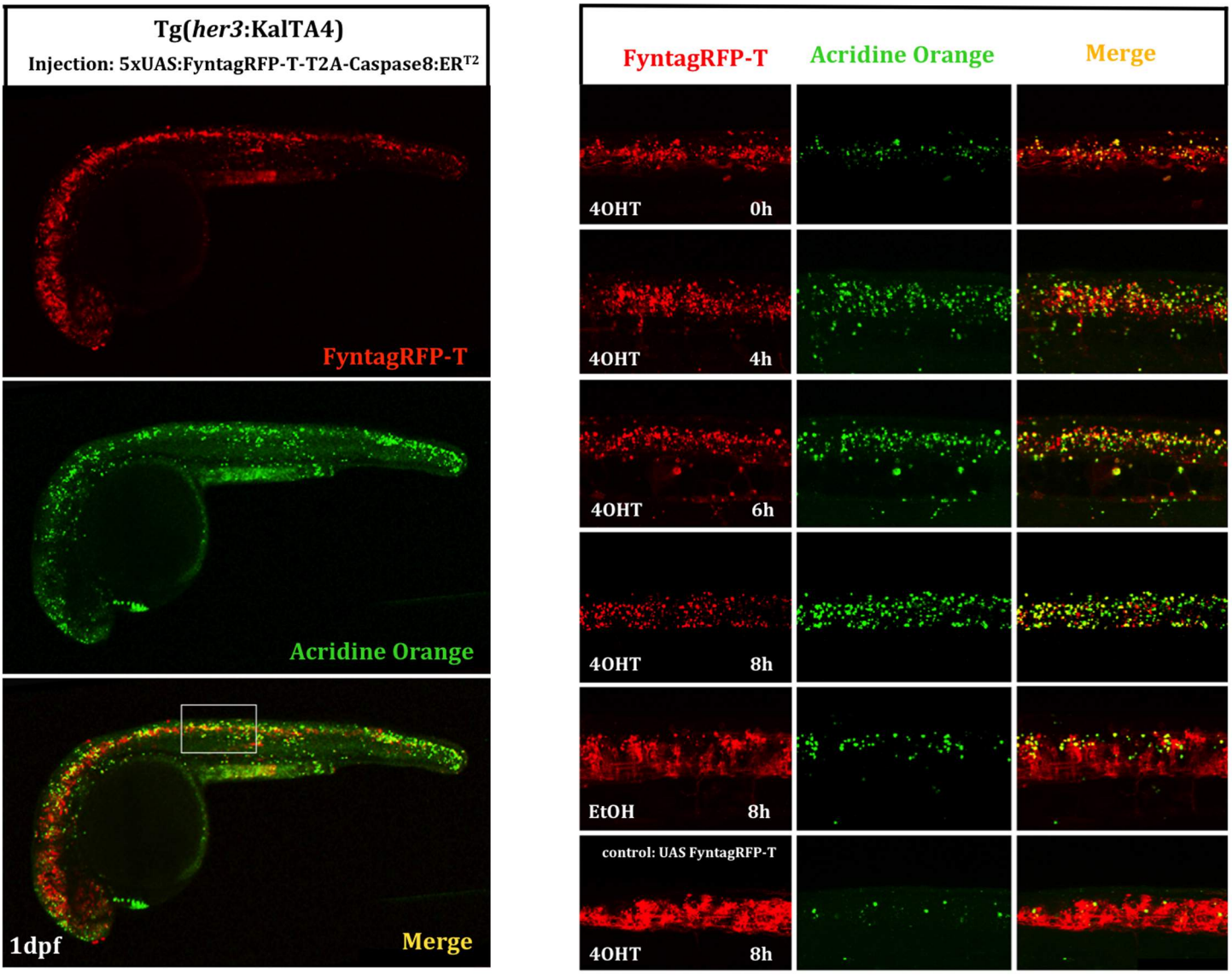

Figure S2: Temporal profile of apoptosis induction by inducible caspase.
Heterozygous Tg(*her3:*KalTA4)^{hzm9Tg} embryos were injected at the one cell stage with a plasmid carrying 5xUAS:FynTagRFP-T-T2A-Caspase8ER^{T2}, followed by acridine orange staining on injected embryos at 24hpf. (A) Gal4/UAS-mediated tissue specific gene expression results in red fluorescent FyntagRFP-T positive cells throughout the ventral central nervous system including the brain, the spinal cord and the retina. Green fluorescent acridine orange staining was used to detect dying cells. To follow the time course of induction of apoptosis a region in the spinal cord marked by a white rectangle was analyzed at higher magnification. (B) In this spinal cord domain the number of green fluorescent dying cells (column in the middle) is increasing upon 4OHT treatment reaching highest levels around 8 hours after initiation of Tamoxifen incubation. Compared to normal developmental levels of apoptosis in embryos injected with the control plasmid 5xUAS:FynTagRFP-T (6th row), 5xUAS:FynTagRFP-T-T2A-Caspase8ER^{T2}-injected embryos treated with EtOH showed an increase in apoptotic cell death (5th row) indicating that the activity of the inducible caspase is leaky under transient transgenic conditions, but can be induced to much higher levels of apoptosis upon Tamoxifen-mediated caspase activation (please compare 4th with 5th row).

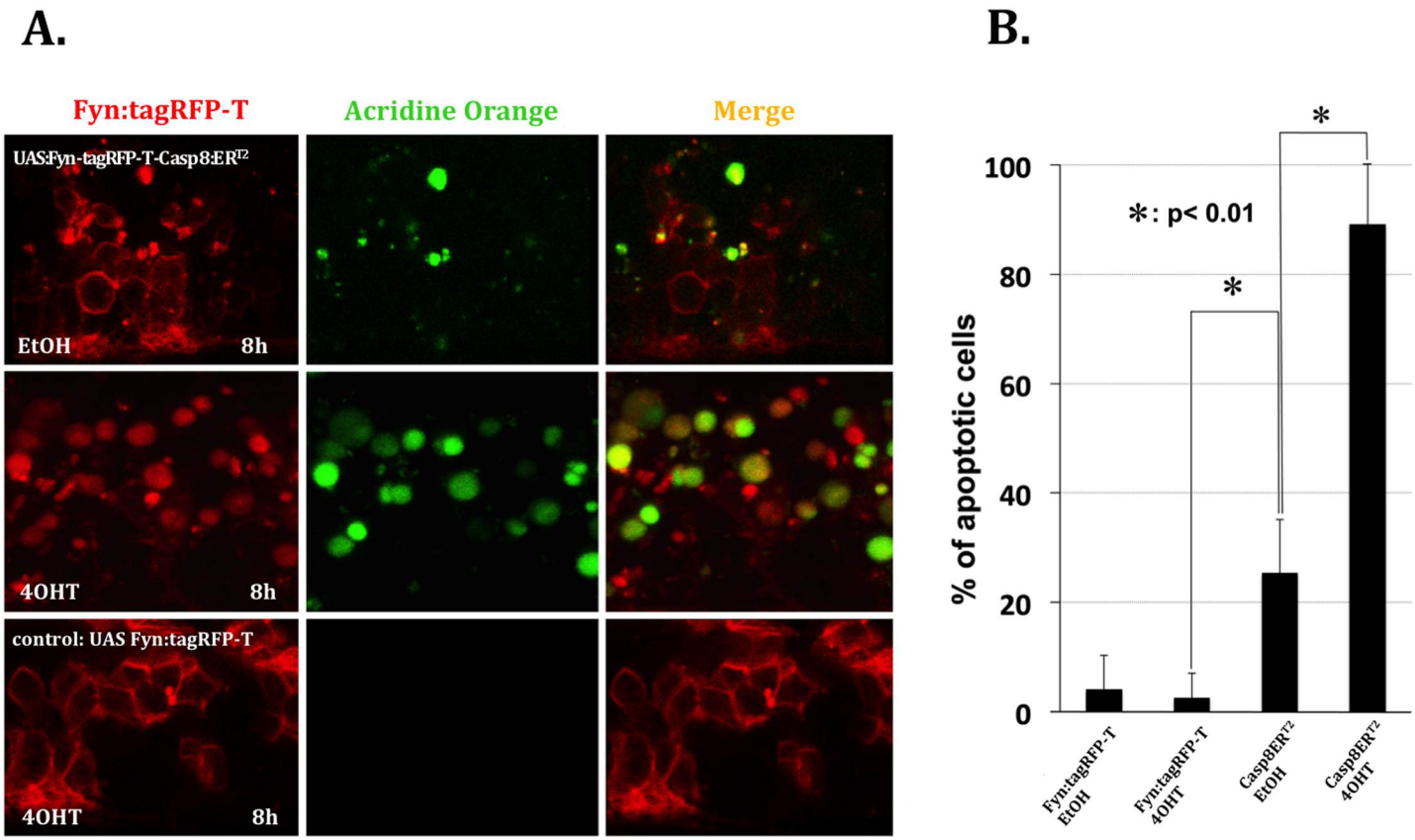

Figure S3: Quantification of induced apoptosis.

(A) Higher magnified images of spinal cord cells expressing FyntagRFP-T/Caspase8ER^{T2} (upper and middle row in A), and control FyntagRFP-T (lower row). Significant induction of apoptosis was observed in almost all FyntagRFP-T expressing cells 8 hours after 4OHT treatment (middle). Compared to control embryos expressing only FyntagRFP-T with virtually no apoptotoc cells (lower row), FyntagRFP-T/Caspase8ER^{T2} -injected embryos treated with EtOH displayed an increased level of apoptosis (upper row) but clearly to a lesser extend than 4OHT treated embryos. (B) Quantification of the percentage of these apoptotic cells was performed by calculating the number of acridine orange/ tagRFP-T double positive cells relative to all tagRFP-T positive cells. Cells were counted on confocal z-stack images through the spinal cord from 5 independent embryos each. * <0.01 : p value is lower than 0.01 by Student´s t-test.

A.

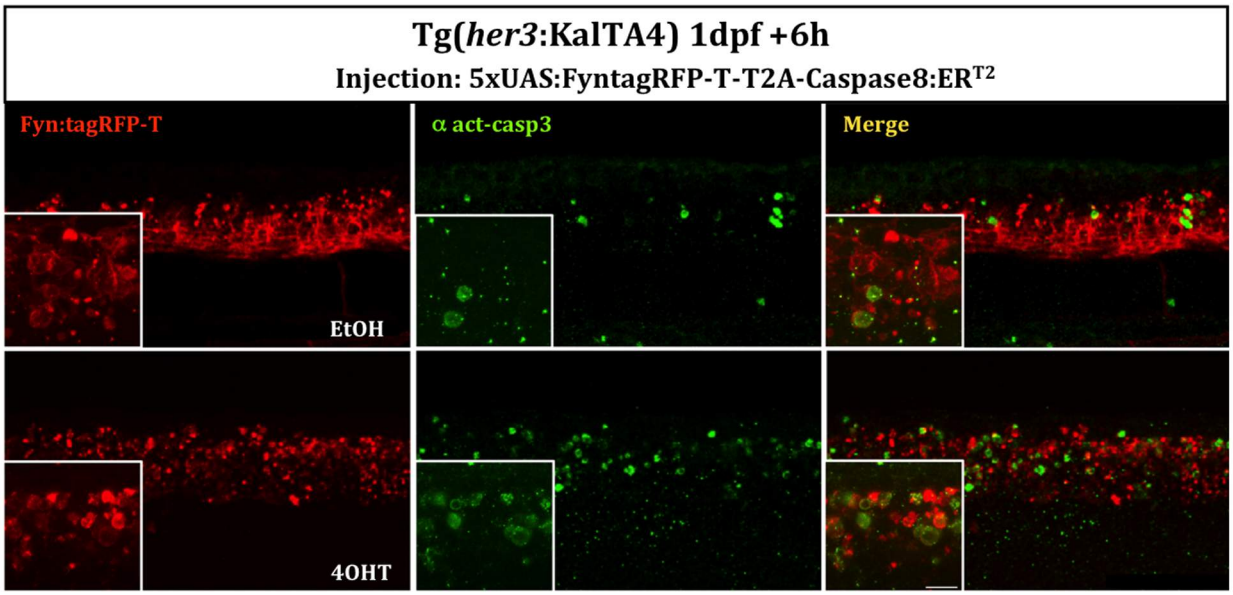

B.

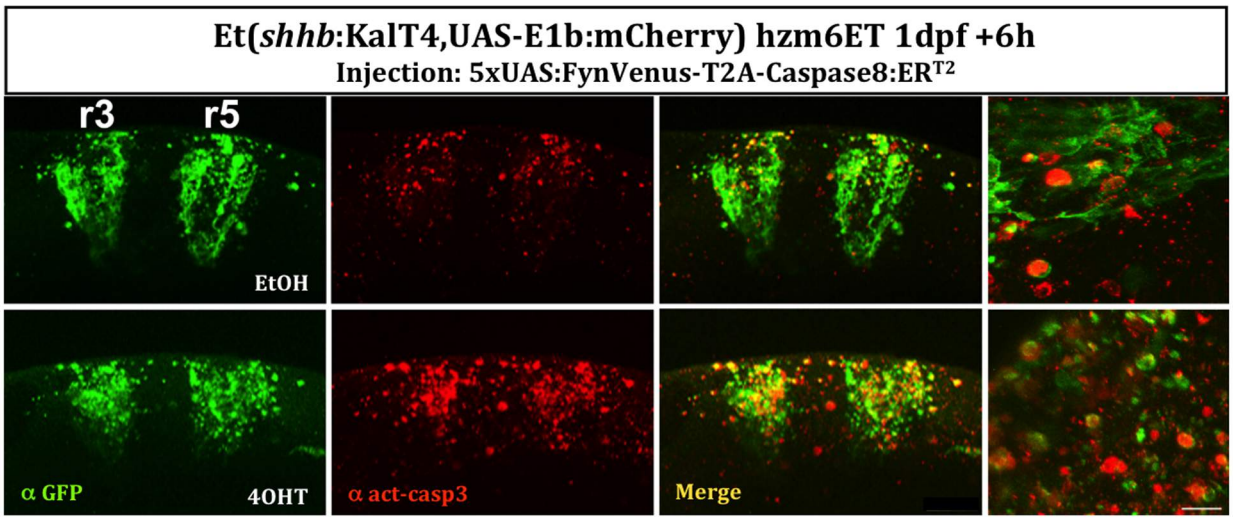

C.

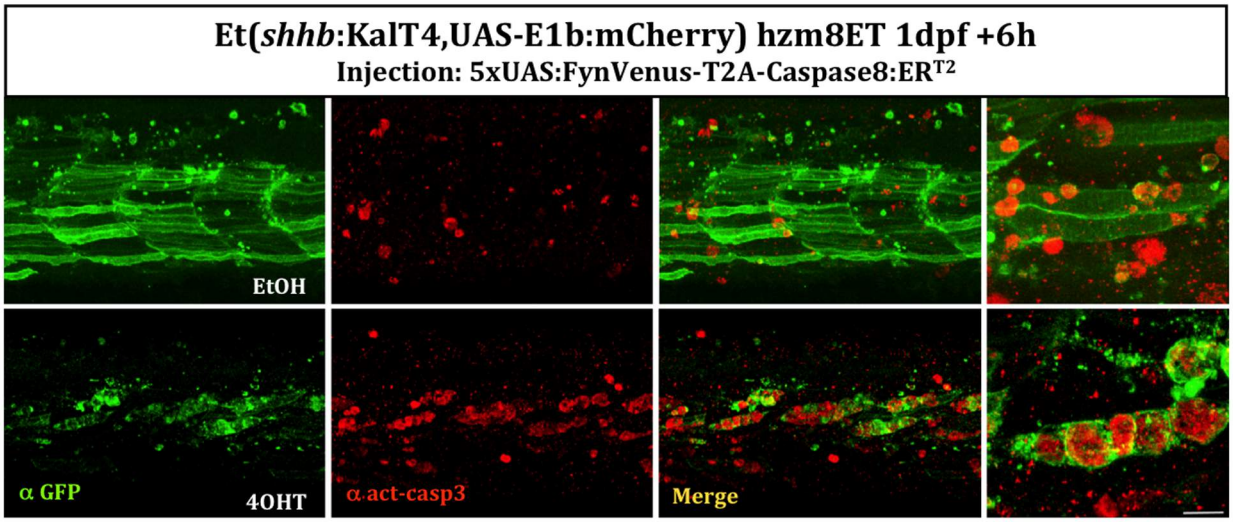

Figure S4: Cell type specificity of apoptosis induction.

Induction of apoptosis in different cells types was investigated by injection of the plasmid 5xUAS:FyntagRFP-T-T2A-Caspase8ER^{T2} (A) or 5xUAS:FynVenus-T2A-Caspase8ER^{T2} (B and C) into embryos of the different KalTA4-expressing driver strains hzm9Tg, hzm6Et and hzm8Et respectively at the one cell stage. At 24hpf injected embryos were treated for 6 hours with either EtOH (upper row) as control or 4OHT (lower row) to induce apoptosis. Subsequently, the embryos were fixed in 4%PFA/PBS and analyzed by immunohistochemistry against activated Caspase3 as indicator of apoptosis. Due to a reduced stability of FynVenus upon fixation, FynVenus expression was enhanced by immunohistchemistry using an anti-GFP antibody. Sacle bar: 50μm; 10μm for insets and highly magnified images.

(A) Tg(*her3:*KalTA4)^{hzm9} embryos injected with 5xUAS:FyntagRFP-T-T2A-Caspase8ER^{T2} reveal FyntagRFP-T-expressing red fluorescent cells in the ventral spinal cord with elevated levels of apoptosis marked by green fluorescent detection of activated Caspase3 compared to EtOH-controls.

(B) hzm6Et embryos driving KalTA4-expression under control of the *krox20* enhancer throughout rhombomere 3 and 5 (Distel et al., 2009) injected with 5xUAS:FynVenus-T2A-Caspase8ER^{T2} reveal FynVenus-expressing green fluorescent cells in the hindbrain demarcating rhombomere 3 and 5 with elevated levels of apoptosis marked by red fluorescent detection of activated Caspase3 compared to EtOH-controls.

(C) hzm8Et embryos driving KalTA4-expression under control of an unkown skeletal muscle enhancer (Distel et al., 2009) injected with 5xUAS:FynVenus-T2A-Caspase8ER^{T2} reveal FynVenus-expressing green fluorescent cells in muscles along the trunk with elevated levels of apoptosis marked by red fluorescent detection of activated Caspase3 compared to EtOH-controls.

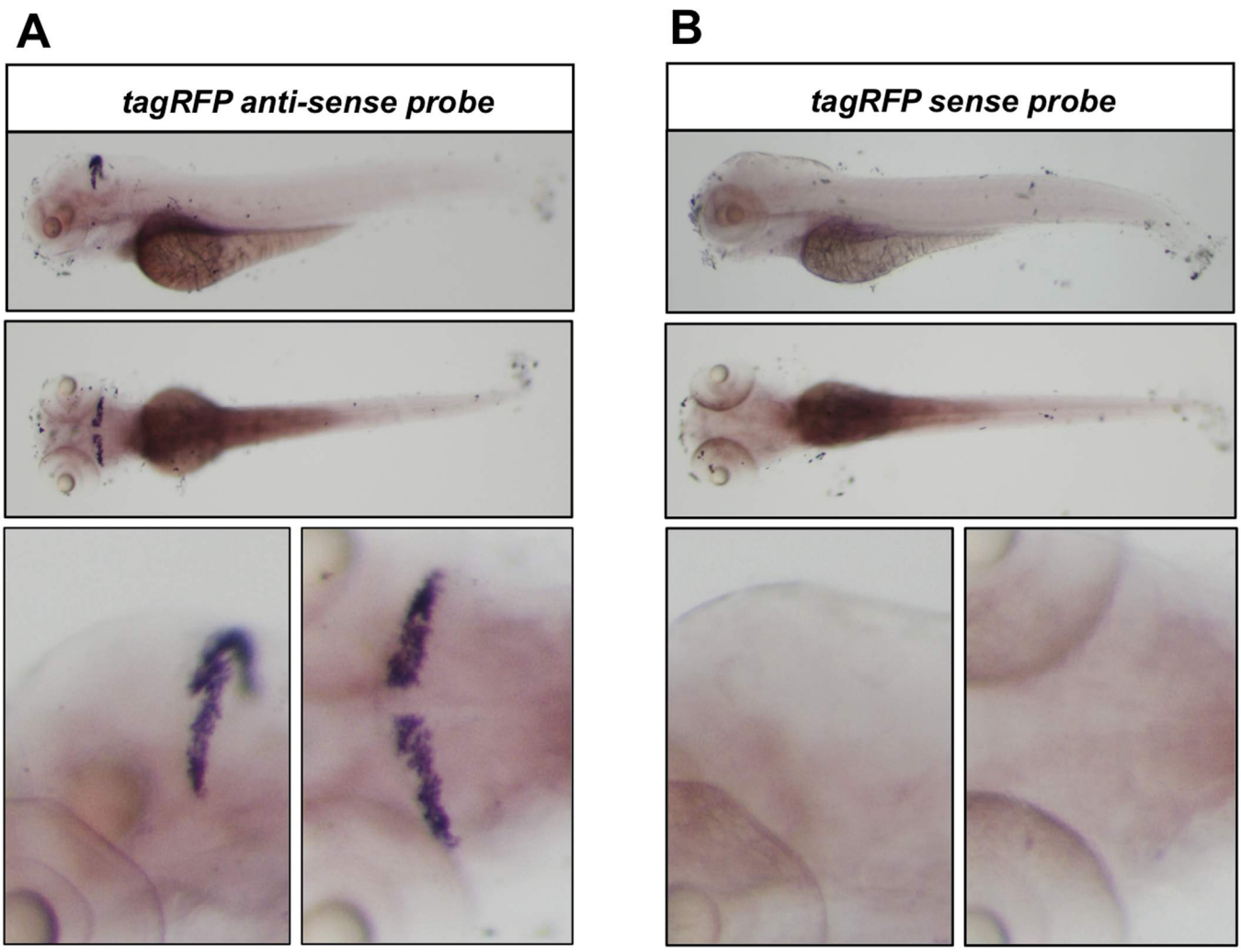

Figure S5: Transgene expression is confined to the cerebellum.
(A) *In situ* hybridization analysis on 4dpf old larvae from the stable transgenic PC-ATTAC™ strain revealed that mRNA for *tagRFP* is exclusively expressed in the cerebellum. (B) PC-ATTAC™ larvae hybridized with the sense probe were used as control.

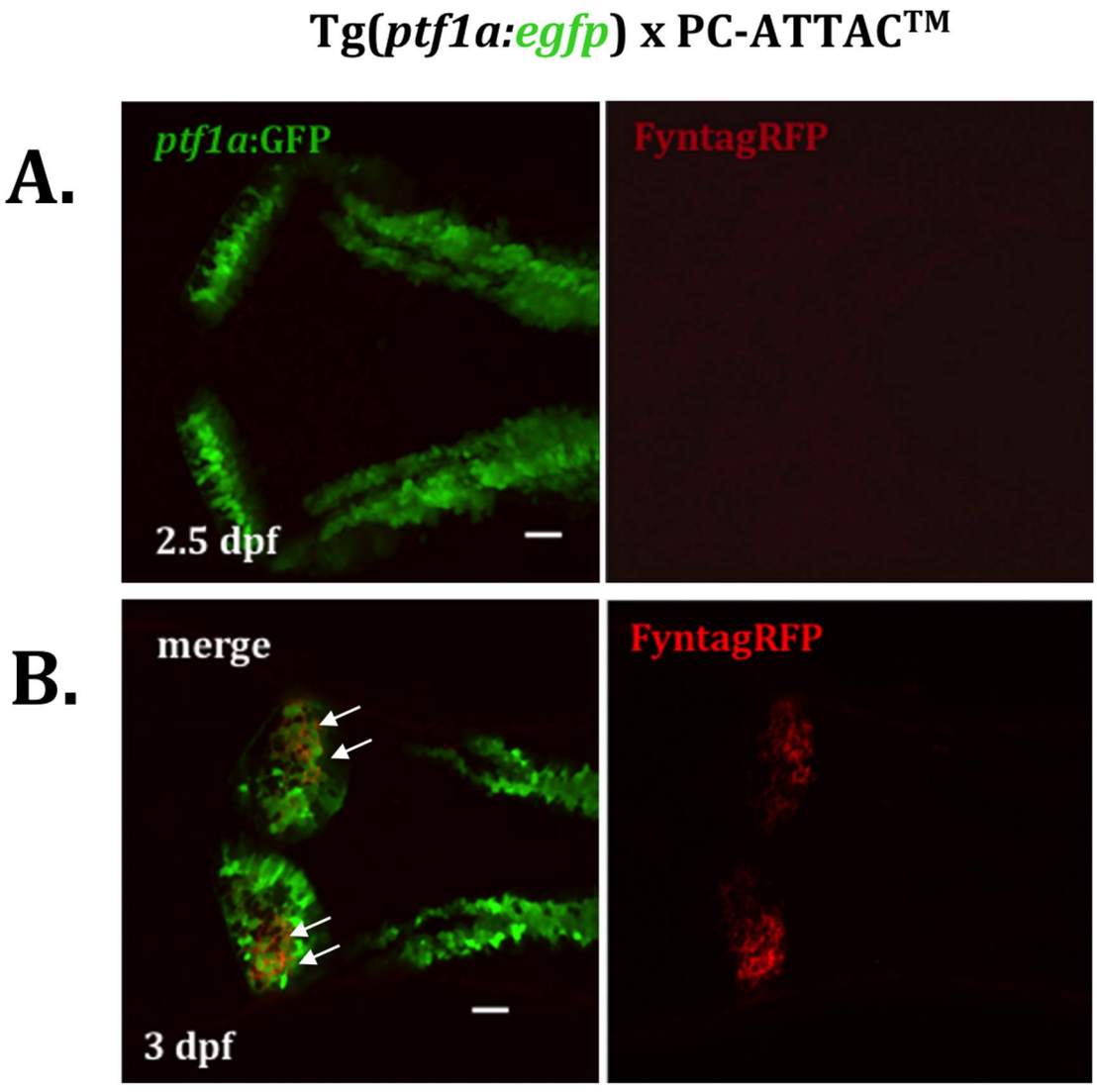

Figure S6: Expression of inducible Caspase8ER^{T2} is initiated in differentiating cerebellar Purkinje cells at around 3 dpf.

Dorsal views of the cerebellum of double transgenic PC-ATTAC™ larvae in the Tg(*ptf1a*:*egfp*) background recorded by confocal laser scanning microscopy. (A) While the GFP-expressing GABAergic progenitor cells were readily visible in the wing-like structures of the cerebellar primordium at 2.5dpf red fluorescent Purkinje cells expressing the inducible Caspase8ER^{T2} were not yet detectable. (B) At 3 dpf numerous red fluorescent differentiating Purkinje cells had appeared co-expressing GFP (white arrows), which is consistent with the previous finding that Purkinje cells are derived from cerebellar GABA-ergic progenitors (Hibi and Shimizu, 2012). Thus the inducible Caspase8ER^{T2} becomes expressed between 2.5 and 3dpf respectively in transgenic PC-ATTAC™ larvae. Scale bar: 20μm.

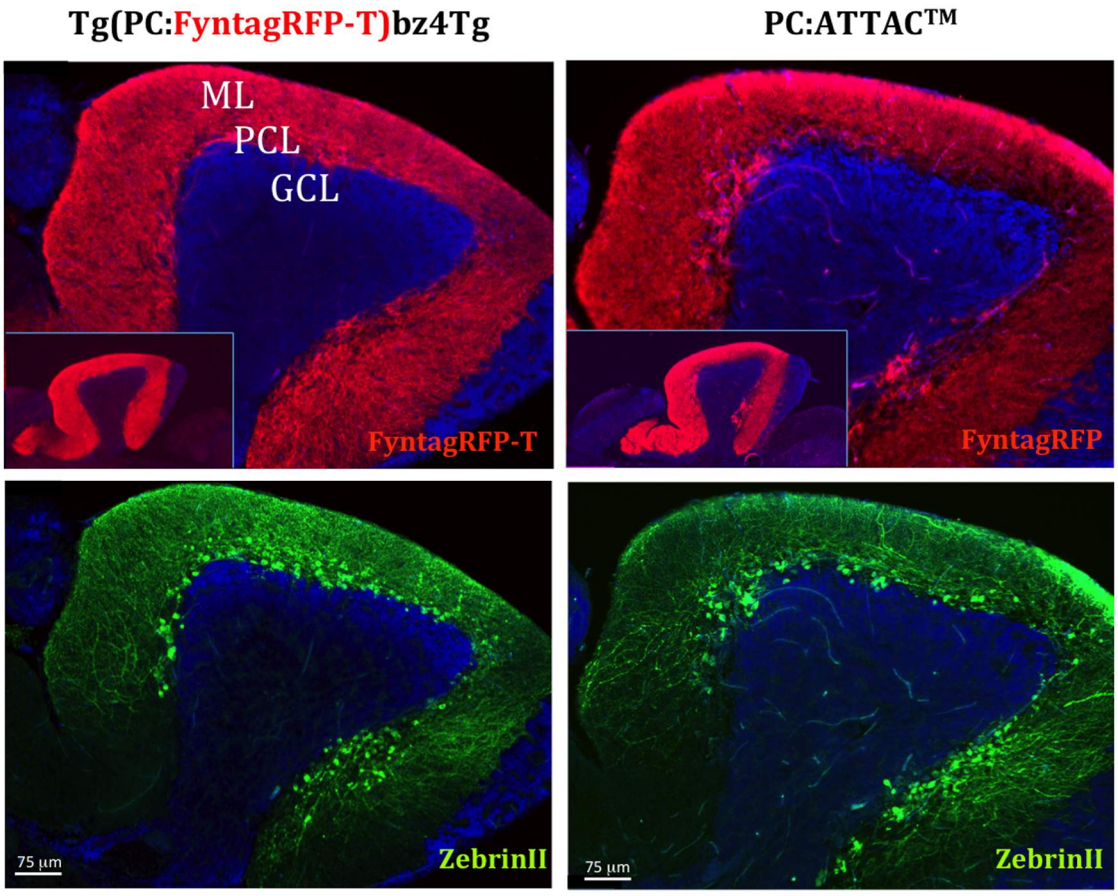

Figure S7: Integrity of Purkinje cell layer in PC-ATTAC™ adults.
Immunohistchemical detection of Purkinje cell specific FyntagRFP and ZebrinII expression on sagittal sections through the cerebellum of adult fish older than 15 months from the control Tg(PC:FyntagRFP-T)^{bz4Tg} (left) and the PC-ATTAC™ (right) strains. Both lines showed intensive FyntagRFP-T/FyntagRFP expression respectively without any signs of dendritic atrophy (upper row, red fluorescence, insets display overview over entire cerebellum), and ZebrinII expression (lower row, green fluorescence) revealed that no apparent Purkinje cell loss was observed in the PC-ATTAC™ cerebellum compared to controls. DAPI was used as counter stain (blue fluorescent signals). Abbr.: GCL: granule cell layer, ML: molecular layer, PCL: Purkinje cell layer. Scale bar: 75µm.

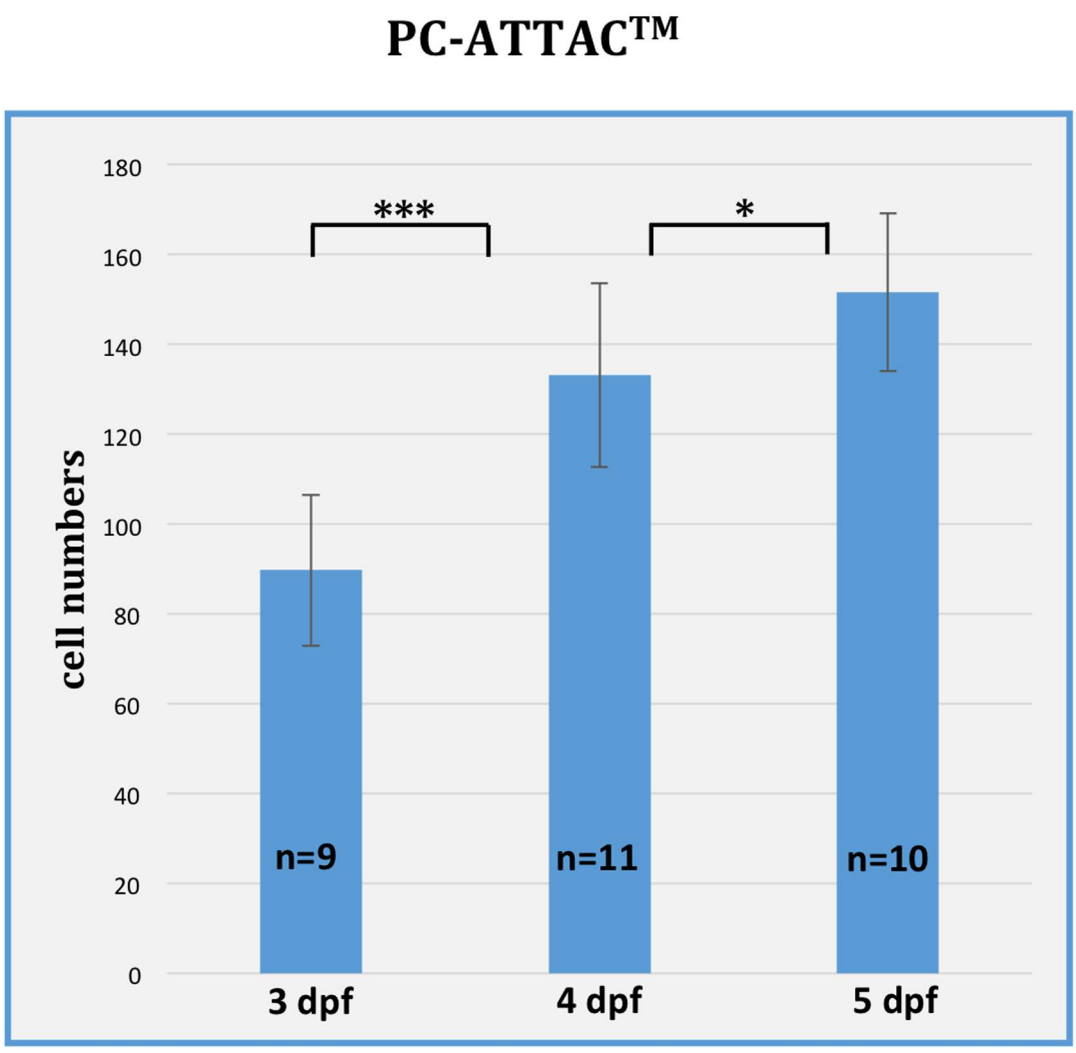

Figure S8: Purkinje cell number in zebrafish larvae.

The graph shows the average number of FyntagRFP expressing cells, which were counted using confocal microscopy sections from one cerebellar hemisphere of PC-ATTAC™ larvae at 3, 4 and 5dpf, revealing that the number of Purkinje cells increases during larval development until 5dpf, reaching a plateau at around 6dpf (Hamling et al., 2015). ***<0.001, *<0.05 : each p value is lower than 0.001, or 0.05 by Student´s t-test, respectively.

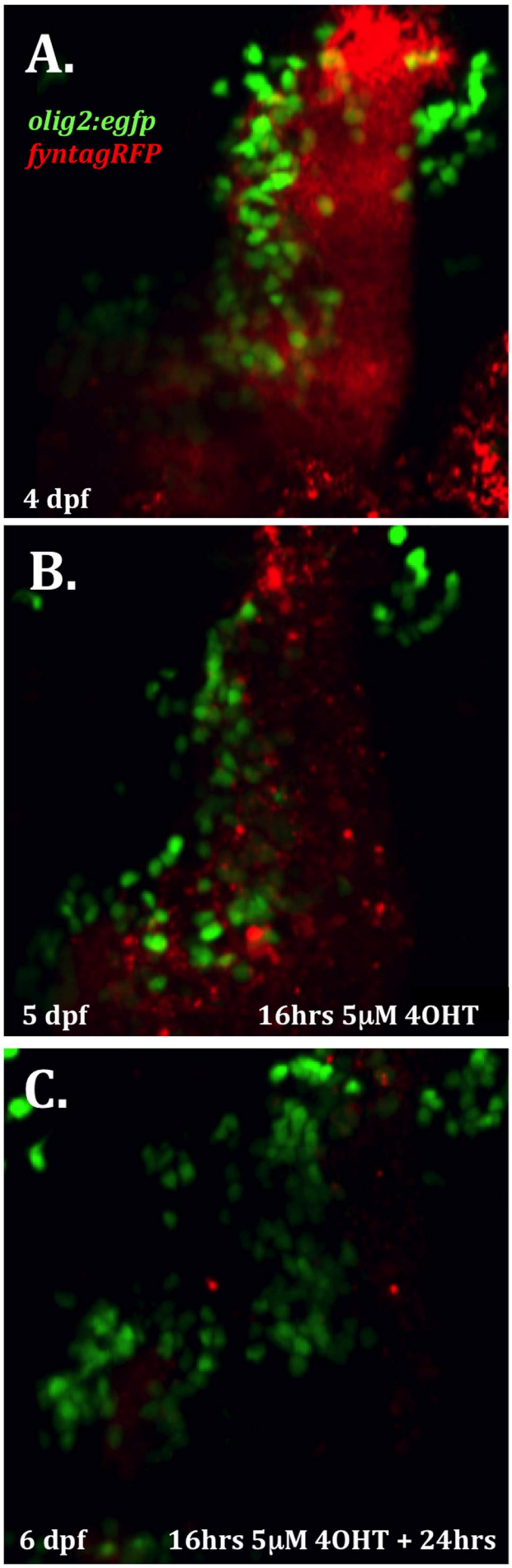

Figure S9: Eurydendroid cells are largely unaffected by PC apoptosis.
Double transgenic PC-ATTAC™ larvae crossed into Tg(*olig2:egfp*) background were subjected at 4dpf to 4OHT treatment to examine the effect of Purkinje cell ablation on *olig2*:*egfp* expressing green fluorescent eurydendroid cells. (A) CLSM image of right cerebellar hemisphere of 4dpf larva showed intact FyntagRFP-expressing Purkinje cells (red) and eurydendroid cell somata (green). (B and C) 4OHT-induced Purkinje cell ablation resulted in the significant reduction of FyntagRFP fluorescence over time (B) at 5dpf directly after the 16hrs of 4OHT-treatment or (C) at 6dpf 24 hours after the 4OHT-treatment was finished, respectively. Green fluorescent eurydendroid cells (ECs) instead were not affected by the Purkinje cell ablation over the whole duration of observation.